

## A LATE CRETACEOUS (MAASTRICHTIAN) AVIFAUNA FROM THE MAEVARANO FORMATION, MADAGASCAR

PATRICK M. O'CONNOR<sup>\*1</sup> and CATHERINE A. FORSTER<sup>2</sup>

<sup>1</sup>Department of Biomedical Sciences, Ohio University College of Osteopathic Medicine, 228 Irvine Hall, Athens, Ohio 45701, U.S.A., oconnorp@ohio.edu;

<sup>2</sup>Department of Biological Sciences, 2023 G Street, NW, The George Washington University, Washington, D.C. 20052, U.S.A., forster@gwu.edu

**ABSTRACT**—Recent field efforts in the Mahajanga Basin of northwestern Madagascar have recovered a diverse Late Cretaceous terrestrial and freshwater vertebrate fauna, including a growing diversity of avialans. Previous work on associated bird skeletons resulted in the description of two named avialans (*Rahonavis*, *Vorona*). Other materials, including two synsacra and numerous appendicular elements, represent at least five additional taxa of basal (non-neornithine) birds. Among the materials described herein are two humeri tentatively referred to *Rahonavis* and numerous elements (e.g., humeri, ulnae, tibiotarsi, tarsometatarsi) assigned to *Vorona*. A near-complete carpometacarpus exhibits a minor metacarpal that exceeds the major metacarpal in length, documenting an enantiornithine in the fauna. Moreover, two additional, small humeri, an ulna, a femur, and a tarsometatarsus also compare favorably with enantiornithines. Finally, two other isolated humeri and a synsacrum are referable to Ornithurae. The latter specimen is notable in the presence of distinct, transversely oriented lumbosacral canals along the inner surface of the bony neural canal. This reveals for the first time a hard-tissue correlate of an anatomical specialization related to increased sensorimotor integration, one likely related to the unique form of avialan bipedal locomotion. Bird fossils recovered from the Maevarano Formation document one of the most size- and phylogenetically diverse Cretaceous-age Gondwanan avifaunas, including representative (1) basal pygostylian, (2) enantiornithine, (3) nonenantiornithine, ornithothoracine, and (4) ornithurine taxa. This Maastrichtian avifauna is notable in that it demonstrates the co-existence of multiple clades of basal (non-neornithine) birds until at least the end of the Mesozoic.

**MALAGASY ABSTRACT (FAMINTINANA)**—Ireo fikarohana natao tao amin'ny Debok' i Mahajanga tany amin'ny faritra avaratra andrefan'i Madagasikara dia nahita karazam-biby an-tanety sy trondron-dranomamy misy taolan-damosina tamin'ny vanim-potoanan'ny Crétacées Aoriana ka anisan'ireny ny fisian'ny ireo vorona (avialans) mbola eo an-dalam-pisandrahana. Ny asa fikarohana teo aloha natao tamin'ireo taolam-borona natambatra dia nafahana nanadihady ireo vorona roa (*Rahonavis*, *Vorona*). Ireo taolana hafa ka anisan'ireny « synsacra » roa sy fivontosana maro isan-karazany, izay milaza ny fisihan'ireo karazam-borona dimy tena hafa tanteraka ka tsy ao amin'ny fianakavian'ny Neornithinae. Anisan'ireo vokampikarohana hita ka nanaovana fanadihadiana dia nahita taolana lavan'ny tana misy ahitana fitovizana amin'i *Rahonavis* sy hafa maro koa (ohatra : taolan-tanana toy ny hita amin'ny sandry (humerus), lanton-tsandry (ulnae), sy tongotra toy ny talondranjo sy vodi-tongotra (tibiotarse, tarsometatarse) izay iraisany amin'ny *Vorona*. Nahitana koa taolam-pela-tanana efa saika feno tanteraka dia ny « carpometacarpe » mampiseho tsy fitoviana eo amin'ny halavan'ny taolana kely (minor) amin'io kanefa lehibe noho an'ny major, mampahantatra ny fisian'ny « enantiornithine » eo amin'ny biby. Ankoatr'izay dia misy taolana roa fanampiny toy ny taolan-tanana dia ny sandry sy lanton-tsandry sy taolan-tongotra iray dia ny taolam-pe (femur) ary taolampelan-tongotra « tarsometatarsi » koa ahahana nampitaha tsara amin'ny « enantiornithines ». Farany dia nahitana taolan-tsandry mitokana roa sy « synsacrum » maneho fitoviana amin'ny Ornithurae. Ny vokatra hita taorina dia nahitana mazava ny fisian'ny fivelaran'ny fantsona “lumbosacral” manaraka ny lalan'ny fantson'ny taolana mitondra ny ritsika. Io tranga io dia mampatsiahy ny fahitana voalohany ny fisian'ny rary matevina maneho ny firafitry ny vatana manana asa voatokana eo amin'ny fampitomboana fiasan'ny ritsika, izay endrika mampiavaka ny vondron'ireo vorona mamindra amin'ny tongotra roa rehefa mihetsika. Ireo vorona fahagola hita tao amin'ny Forona Maevarano dia nahitana ny iray amin'ny goavana indrindra sy maro fisandrahana ara-pivoarana (phylogenetique) ny biby vorona avy tamin'ny Gondwana tamin'ny vanim-potoanan'ny Crétacées, ka anisan'izany (1) pygostylian fototra, (2) enantiornithines, (3) tsy enantiornithine, ornithothoracine, ary (4) vondrona ornithurine. Io biby vorona Maastichtian io dia mampiseho mazava ny fisian'ny ireo karazam-borona isan-karazany (tsy neornithine) hatramin'ny faran'ny Mesozoïque farafaharatsiny.

### INTRODUCTION

Recent discoveries of Mesozoic avialan fossils have substantially increased our knowledge of the origin and initial radiation of the clade (Hou et al., 1996; Chiappe et al., 1999, 2001; Chiappe and Dyke, 2002; Chiappe and Witmer, 2002; Zhou and Zhang, 2003). Moreover, such discoveries, along with those of a number of nonavialan theropods, have (1) helped delineate the phylogenetic position of basal birds among the latter group (e.g., Chiappe, 2002; Clark et al., 2002), (2) demonstrated a previously un-

derappreciated ecological diversification of avialans during the Mesozoic (Serenó and Rao, 1992; Chiappe, 1995; Sereno, 2000; Zhou and Zhang, 2000, 2002, 2005; Hou et al., 2004; Lamanna et al., 2006; You et al., 2006; Zhou et al., 2008), and (3) in some cases, shed light on the origin of modern (neornithine) birds (Hope, 2002; Kurochkin et al., 2002; Mayr and Clarke, 2003; Dyke and van Tuinen, 2004; Clarke et al., 2005).

Notably diverse Mesozoic avifaunas include those from the Lower Cretaceous Yixian and Jiufotang formations in Liaoning Province, northeast China (e.g., Ji et al., 1999; Zhou and Zhang, 2003), the Upper Cretaceous Djadokhta, Barun Goyot, and Nemegt formations in Mongolia (Norell and Clarke, 2001; Clarke

\*Corresponding author.

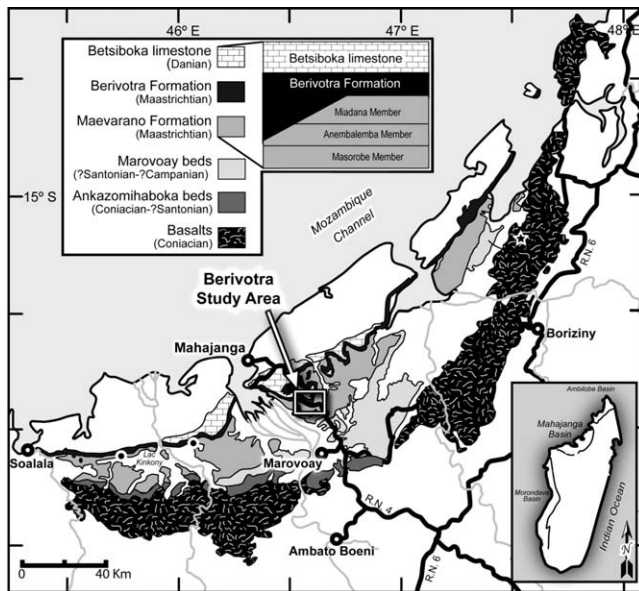


FIGURE 1. Map illustrating the location of the Mahajanga Basin and exposures of the Maevarano Formation in northwest Madagascar. The white box highlights the Berivotra Study Area of the Mahajanga Basin Project, the area where the described avialan fossils were discovered.

and Norell, 2002, 2004), the Upper Cretaceous Rio Colorado and Lecho formations in South America (Chiappe, 1993, 1996a, 1996b), and to a lesser extent, the enantiornithine avifauna from the Early Cretaceous Las Hoyas locality in Spain (Sanz, 1992; Sanz et al., 1995, 1996, 1997). Other locales from throughout Asia, Europe, and North America also preserve relatively limited, yet important, avialan fossils (e.g., Buffetaut et al., 1995; Varricchio and Chiappe, 1995; Chiappe et al., 2002). See Gauthier and Gall (2001), Chiappe and Dyke (2002), and Chiappe and Witmer (2002) for recent overviews on Mesozoic bird evolution.

To date, avialan fossils recovered from South America, particularly Argentina, represent the most diverse avifauna yet collected from Cretaceous strata in the southern hemisphere (e.g., Chiappe, 1996a; Chiappe and Dyke, 2002). Other Gondwanan occurrences of Cretaceous age avialan fossils are known from only a restricted number of specimens, including those recovered from localities in Australia (Molnar, 1986), Afro-Arabia (Dalla Vecchia and Chiappe, 2002), and the Antarctic Peninsula (Noriega and Tambussi, 1995; Clarke et al., 2005).

Two taxa, *Vorona berivotrensis* (Forster et al., 1996, 2002) and *Rahonavis ostromi* (Forster et al., 1998), have been described from the Upper Cretaceous [Maastrichtian] Maevarano Formation (Rogers et al., 2000) exposed in the Mahajanga Basin, northwestern Madagascar (Fig. 1). The holotype specimens of both taxa were recovered from a single locality, MAD 93-18, and, although only represented by partial skeletons, further documented the growing diversity of avialans on southern hemisphere landmasses during the Cretaceous Period.

*Vorona berivotrensis*, a relatively large form (tibiotarsus length ~166 mm) erected on the basis of associated hind limb elements (Forster et al., 1996), has variously (and more or less rigorously) been placed (1) within Enantiornithes (e.g., Feduccia, 1999), (2) in an unresolved polytomy that includes Enantiornithes and a clade consisting of the South American *Patagopteryx* and Ornithurae (Forster et al., 1996), (3) in an unresolved polytomy [node defined as Ornithuromorpha] that includes *Patagopteryx* and Ornithurae to the exclusion of Enantiornithes (Chiappe, 2002), or (4) as the sister taxon to Ornithurae (Zhou et al., 2008).

The dynamic phylogenetic placement of *Vorona* no doubt relates to the limited number of informative characters preserved on the holotypic (UA 8651) and referred (FMNH PA 715, FMNH PA 717) specimens.

*Rahonavis ostromi*, based on a single associated postcranial skeleton (UA 8656), was originally assigned a basal position among birds, often as the sister taxon to *Archaeopteryx lithographica* (e.g., Forster et al., 1998; Chiappe and Dyke, 2002). In contrast, recent analyses examining the position of newly discovered nonavian theropods (e.g., *Tsaagan*, *Buitreraptor*) within Maniraptorata have questioned the avialan status of *Rahonavis*, instead suggesting that it represents a dromaeosaurid (Makovicky et al., 2005; Norell et al., 2006; Novas et al., 2008). However, these analyses have included only a limited number of avialan taxa that would be critical for rigorously evaluating the phylogenetic position of *Rahonavis*. Nonetheless, a monographic treatment of *Rahonavis* is currently in preparation and will provide a detailed description of the specimen, including previously undescribed elements of the skeleton and subsequent studies will no doubt clarify the phylogenetic position of *Rahonavis* among maniraptoran nonavian and basal avialan theropods. For the purpose of this paper, *Rahonavis* will be considered along with the Maevarano avifauna.

Although *Vorona* and *Rahonavis* represent the most complete birds from the Maevarano Formation, they represent only a fraction of the avialan taxa recovered to date. A diversity of other forms, represented predominantly by isolated elements, has also been recovered from the formation. Because of the incomplete and isolated nature of the avialan material described herein, coupled with a limited ability to definitively refer these materials to either of the two named taxa (*Vorona* and *Rahonavis*), these specimens will not be named in this paper but will be referred to by specimen number. Finally, although many of the specimens are incomplete, the bone surface is well preserved, as is the case with most fossils recovered from the Maevarano Fm., and often reveals important aspects of anatomy. In sum, the developing avifauna from the Maevarano Formation constitutes not only the most diverse assemblage of birds known from Africa and its surrounding islands during the Cretaceous, or indeed the Mesozoic, but features a diversity that parallels that known only from Lower Cretaceous deposits (e.g., Yixian and Jiufotang formations) in China.

## MATERIALS AND METHODS

All specimens were examined via stereomicroscopy and measured on a Nikon SMZ-1500 stereomicroscope equipped with a Cooled Insight Color camera bundled with Spot 4.06 Imaging software. Micro-computed tomography was completed for selected specimens on a GE eXplore Locus MicroCT Scanner at the Ohio University MicroCT Facility, and resulting scan data was reconstructed in Amira 4.1.1.

**Institutional Abbreviations**—FMNH, Field Museum of Natural History, Chicago, Illinois; IGM, Institute of Geology, Mongolia, Ulan Bataar; IVPP, Institute of Vertebrate Paleontology and Paleoanthropology, Beijing, People's Republic of China; PVL, Instituto-Fundación Miguel Lillo, Tucumán, Argentina; UA, Université d'Antananarivo, Antananarivo, Madagascar.

**Anatomical Nomenclature and Abbreviations**—Nomenclature used throughout is based on anglicized versions of standardized terms from Handbook of Avian Anatomy: Nomina Anatomica Avium (Baumel, 1993) and from Livezey and Zusi (2006). Abbreviations are included in figure captions.

**Age and Distribution**—All specimens described herein were recovered from the Anembalemba Member (Rogers et al., 2000) of the Maevarano Formation (Maastrichtian, Upper Cretaceous), Mahajanga Basin (Berivotra Study Area), northwestern

Madagascar (Fig. 1). The Anembalemba Member is interpreted as having accumulated during large-scale, sand-sized debris flows originating as a result of exceptional, yet intermittent, rainfall events (Facies 1), and during relatively quiescent periods of low stream discharge (Facies 2) in a semi-arid, seasonal environment (Rogers, 2005). See Rogers et al. (2000) and Rogers (2005) for additional stratigraphic and sedimentologic details pertaining to deposition of the Maevarano Formation.

**Described Material**—FMNH PA 741 (large synsacrum), UA 9601 (small synsacrum), UA 9602 (left coracoid), FMNH PA 779 (left coracoid), FMNH PA 742 (partial furcula), UA 9603 (partial furcula), FMNH PA 743 (partial left humerus-Taxon A), FMNH PA 744 (right humerus-Taxon A), FMNH PA 745 (distal right humerus-Taxon A), UA 9749 (partial left humerus-Taxon A), UA 9750 (partial left humerus-Taxon A), FMNH PA 746 (distal left humerus-Taxon B), UA 9604 (distal right humerus-Taxon B), FMNH PA 747 (right humerus-Taxon C), UA 9605 (proximal left humerus-Taxon D), UA 9606 (right humerus-Taxon E), UA 9607 (distal right humerus), FMNH PA 748 (distal left humerus), FMNH PA 749 (left humerus-Taxon F), UA 9751 (left ulna), FMNH PA 750 (left ulna), UA 9608 (proximal right ulna), FMNH PA 751 (proximal [right ?] radius), FMNH PA 780 (left carpometacarpus), FMNH PA 752 (left femur), UA 9609 (distal right tibiotarsus), UA 9752 (proximal left tibiotarsus), FMNH PA 782 (left tarsometatarsus), FMNH PA 753 (left metatarsals III and IV), UA 9610 (right metatarsal I), and UA 9611 (left metatarsal I). See Table 1 for measurements of selected specimens.

## DESCRIPTIONS

**Synsacra**—Two isolated and morphologically distinct synsacra, one large (FMNH PA 741) and one small specimen (UA 9601), were collected from locality MAD 93-18.

FMNH PA 741 is a large (43 mm in length), robust synsacrum that consists of seven fused, ventrally concave vertebrae (Fig. 2A–E), with transverse processes (sacral ribs) that are either absent altogether (S1 to S5 on the right side) or only partially preserved (S3, S4, and S7 on the left side). The element is otherwise well preserved and retains most of its three-dimensional shape. Neural spines are indistinct and represented by a low, midline crest along the dorsal margin of the fused neural arches. Although the crest is visible throughout the length of the element, it is most prominent dorsal to the first four fused vertebrae. The completely fused centra are dorsoventrally compressed (Fig. 2D) and feature smooth ventral and lateral surfaces (Fig. 2B) such that individual vertebrae are only discernable by examining the position and number of their respective transverse processes. The cranial surface of the first vertebra is broad (width approximately twice height) and distinctly procoelous (Fig. 2D). The caudal surface of the seventh synsacral vertebra, although incompletely preserved, appears amphiplatyan. The large neural canal is broader than tall at both the cranial (Fig. 2D) and caudal (Fig. 2E) ends of the synsacrum. And although the dorsoventral-mediolateral proportions of the neural canal remain constant through the length of the synsacrum, the area of the canal reduces by half.

The fused centra exhibit a dramatic reduction in width between positions 2 and 5 before expanding again at position 7 (Fig. 2B). The transverse processes are distinct along the series, possess a flat, yet craniocaudally expanded dorsal surface (Fig. 2A), and are buttressed ventrally by prominent struts (Fig. 2B). The size of the struts varies, being robust at positions 1, 4, and 7, and relatively slender at the other positions. The ventral extent of the transverse processes at positions 4 and 7 nearly reach the ventral margin of their respective centra (Fig. 2C). The major axis of orientation of the transverse processes also varies along the series, with the first three positions oriented craniolaterally, po-

TABLE 1. Measurements (mm) for selected Maevarano Formation avialans.

<hr/>		
Coracoid, Ornithothoraces		
FMNH PA 779	Length	50.1
	Width, sternal end	17.9
	Width, mid-ramus	3.5
	Width, shoulder end	8.6
<hr/>		
Humeral Taxon A (? <i>Vorona</i> )		
FMNH PA 744 (large morph)	Length	120.0*
	DV diameter	9.5
	CrCa diameter	7.7
UA 9750 (small morph)	Length	79.4*
	DV diameter	6.9
	CrCa diameter	4.8
<hr/>		
Humeral Taxon B (? <i>Rahonavis</i> ) <sup>1</sup>		
FMNH PA 746/UA 9604 (left/right sides)	Length	37.8 <sup>†</sup> /48.3 <sup>†</sup>
	DV diameter	7.7*/7.6*
	CrCa diameter	5.4*/5.4*
<hr/>		
Humeral Taxon C		
FMNH PA 747	Length	44.6
	DV diameter	2.7
	CrCa diameter	2.3
<hr/>		
Humeral Taxon D		
UA 9605	Length	38.1 <sup>†</sup>
	DV diameter	3.6
	CrCa diameter	2.7
<hr/>		
Humeral Taxon F		
FMNH PA 749	Length	16.5 <sup>†</sup>
	DV diameter	1.3
	CrCa diameter	1.0
<hr/>		
Ulnae (? <i>Vorona</i> )		
FMNH PA 750 (large morph)	Length	129.0 <sup>†</sup>
	DV diameter	6.2*
UA 9751 (small morph)	Length	93.3
	DV diameter	6.9
<hr/>		
Femur, Enantiornithes		
FMNH PA 752	Length	32.5
	CrCa diameter	2.5
<hr/>		
Tibiotarsi ( <i>Vorona</i> )		
UA 9752 (small morph)	Length	53.5 <sup>†</sup>
	CrCa diameter	4.3
<hr/>		
Tarsometatarsi ( <i>Vorona</i> )		
FMNH PA 782 (small morph)	Length	41.9
	Midshaft width	6.2
<hr/>		

<sup>1</sup>Due to incomplete preservation measurements of the dorsoventral and craniocaudal diameter in Humeral Taxon B were not taken at the element midpoint, but are used merely to provide an estimate of midshaft values.

\*Estimated size; <sup>†</sup>preserved length.

**Abbreviations:** CrCa, craniocaudal; DV, dorsoventral.

sition 4 oriented laterally, and positions 5–7 oriented caudolaterally (Fig. 2A–B). The distal end of the transverse process forms an expanded diapophyseal facet for increased contact with the ilium (Fig. 2C). The extent of this expansion varies, with the largest diapophyses apparent at the cranial and caudal end of the series. The distal ends of the fourth through sixth transverse process (on the left side only due to incomplete preservation of the right side) are united to form a single, irregular contact surface for the ilium (Fig. 2C). The transverse process of the left seventh synsacral vertebra is not preserved; however, based on the fusion of the preserved sixth and seventh diapophyses on the right side of the element, it is likely that at least positions 4–7 were united (Fig. 2C) laterally near their contact with the ilium. Additionally, the ventral margin of fourth transverse process is connected to the dorsal margin of fifth by a lamina of bone.

The total synsacral count of seven co-ossified vertebrae and overall organization of FMNH PA 741 generally resembles the condition in confuciusornithids (Chiappe et al., 1999), *Sapeornis* (Zhou and Zhang, 2003:fig. 4), *Archaeorynchus* (Zhou and Zhang, 2006), and some enantiornithines (e.g., *Protopteryx*,

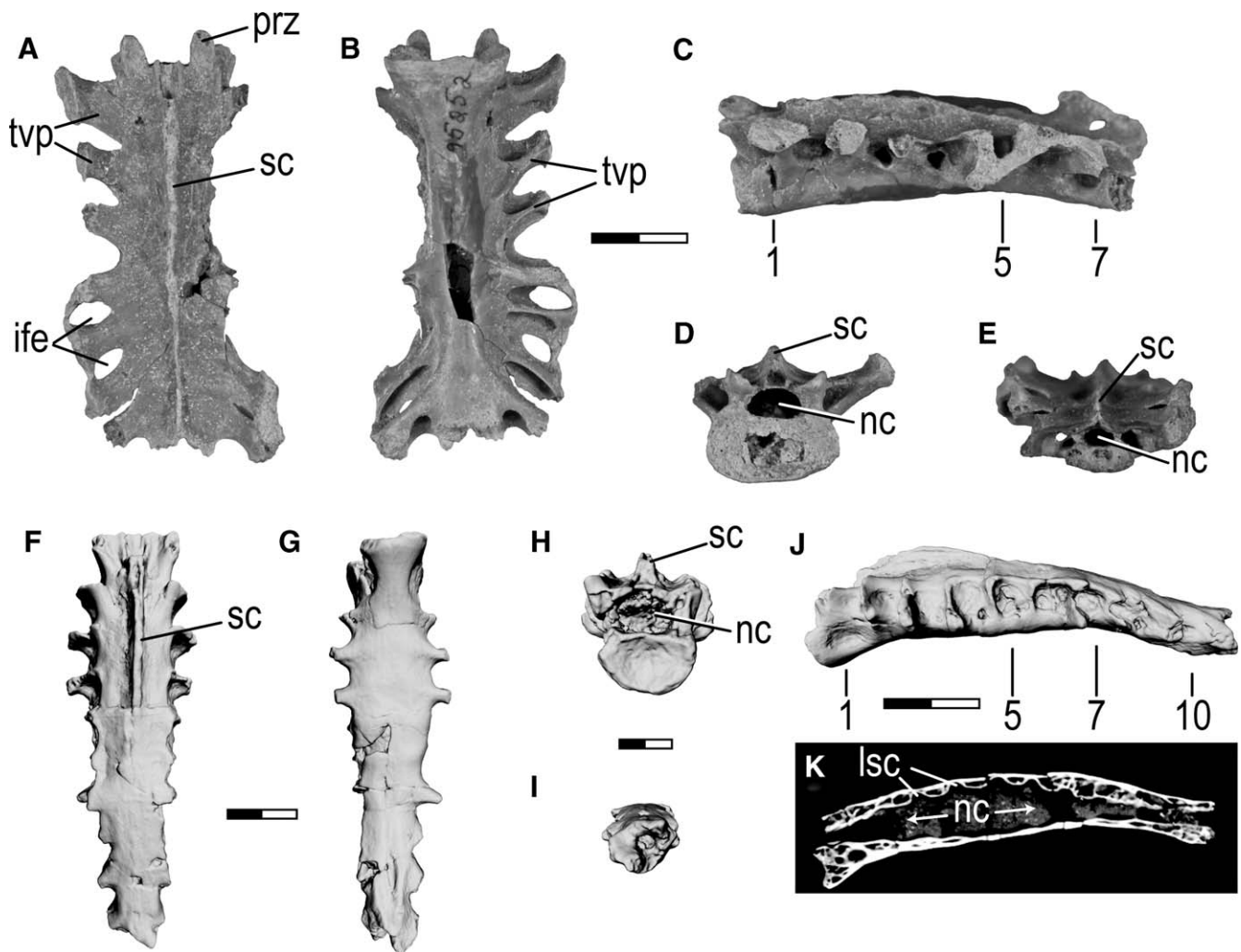


FIGURE 2. Synsacrum (FMNH PA 741) of Avialae indet. in dorsal (A), ventral (B), left lateral (C), cranial (D), and caudal (E) views. Synsacrum of Ornithurae indet. (UA 9601) based on  $\mu$ CT scanning and visualization in dorsal (F), ventral (G), cranial (H), caudal (I), and left lateral (J) views.  $\mu$ CT image of UA 9601 in parasagittal (K) view. **Abbreviations:** ife, intertransverse foramen; lsc, lumbosacral canal; nc, neural canal; prz, prezygapophysis; sc, synsacral crest; tvp, transverse process; numbers 1, 5, 7, and 10 indicate synsacral vertebral position. Scale bar equals 1.0 cm in A–E, 0.5 cm in F–G, 0.2 cm in H–I, and 0.5 cm J–K.

*Pengornis*; Zhang and Zhou, 2000; Zhou et al., 2008), indicating that this taxon occupies a relatively basal position among avialae. Moreover, FMNH PA 741 and *Sapeornis* (IVPP V13275) share the following suite of characteristics: broad sacral transverse processes oriented cranio-laterally in the first three positions, transversely in the fourth position, and caudally in positions 5 through 7; distal ends of the fifth through seventh transverse processes united, thereby forming two pairs of elliptical foramina in the horizontal lamina of the synsacrum (Fig. 2A; Zhou and Zhang, 2003:fig. 4g).

UA 9601 is a small (25 mm in length) synsacrum that consists of 10 fused vertebrae that together form a shallow, ventrally concave arch in lateral view (Fig. 2F–K). Although concave as a unit, it is clear that distinct angulations exist between positions 1 and 3 and between positions 7 and 8 (Fig. 2J). The fused neural arch complex is nearly complete throughout the length of the element, preserving the coalesced pedicles, laminae, and neural spines. The transverse processes are incomplete; however, those preserved along the cranial one-third of the element project laterally, demarcating distinct intertransverse fossae (Fig. 2F–G). The

ultimate two transverse processes, although incomplete, project caudolaterally. Transverse processes are sub-triangular in lateral view, being cranio-caudally expanded at their ventral-most point (Fig. 2J). Finally, synsacral transverse processes are high, being attached along the dorsoventral extent of their respective centra.

Sacral centra are variably shaped and sized (dorsoventrally and mediolaterally) throughout the series, with the widest at positions 3 through 5 (Fig. 2G). Centra exhibit a decrease in all dimensions from positions 6 through 10 such that the terminal unit is merely a thin plate of bone positioned ventral to the neural canal. The cranial articular surface on the first vertebra is concave and dorsoventrally compressed (Fig. 2H). A prominent fossa is present on the lateral surface of the first centrum (Fig. 2J), similar to the condition observed in *Zhyaornis* (Nessov, 1992:fig 2k); however, *Zhyaornis* exhibits a prominent fossa on the lateral surface of the first two synsacral vertebrae. A slender midline spinous crest is developed along the dorsal surface of the first five coalesced neural arches. Caudal to this point, however, the dorsal surface of the fused neural arch complex is flat. The ventral surface of the synsacrum is smooth throughout most of its length,

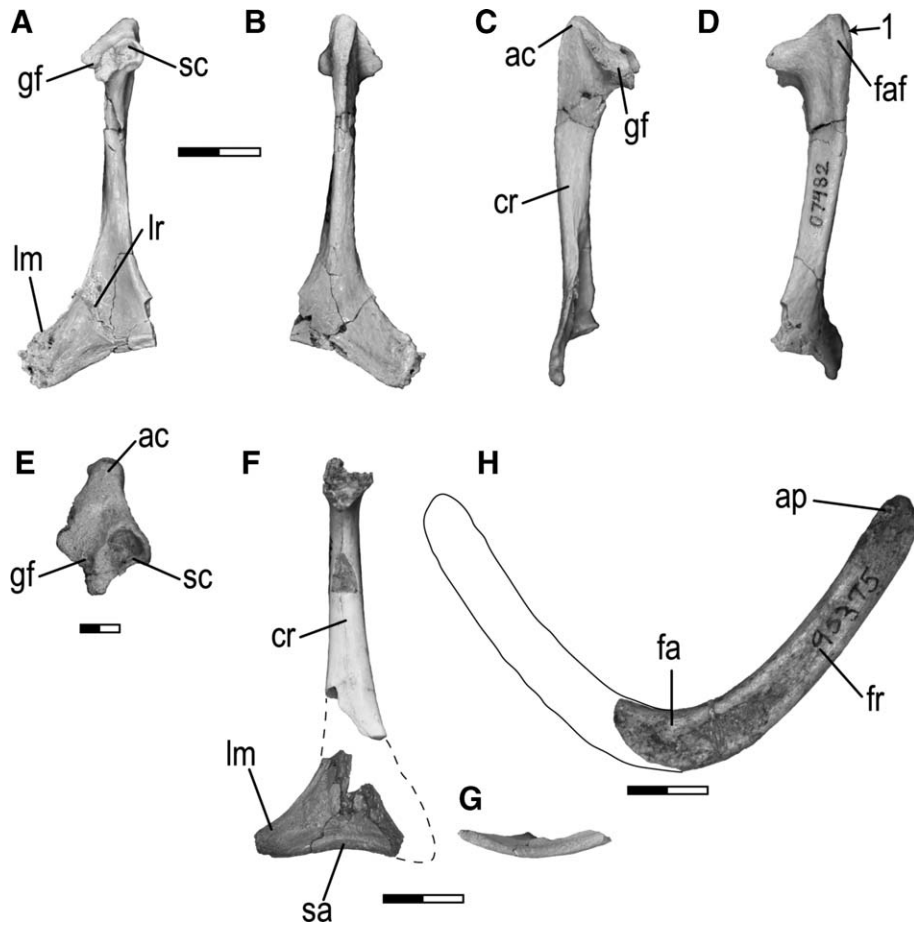


FIGURE 3. Pectoral girdle elements of *Ornithothoraces* indet. Left coracoid (FMNH PA 779) in dorsal (A), ventral (B), lateral (C), medial (D), and proximal (E) views. Left coracoid (UA 9602) in ventral (F) and sternal (~ proximal) (G) views. Partial right furcula (FMNH PA 742) in caudal (H) view. **Abbreviations:** ac, acrocoracoid process; ap, acromial process (clavicular); cr, coracoid ramus; fa, furcular apophysis; faf, furcular articular facet; fr, furcular ramus; gf, glenoid facet; lm, lateral margin; lr, longitudinal ridge; sa, sternal articulation; sc, scapular cotyla; l, longitudinal sulcus on acrocoracoid process. Scale bar equals 1.0 cm in A–D, 0.5 cm in E, 1.0 cm in F, and 0.5 cm in H.

with the development of a shallow midline sulcus visible just ventral to the caudal three positions (Fig. 2G). The neural canal is slightly broader than tall, narrowing considerably from cranial to caudal through the synsacrum.

UA 9601 is here referred to *Ornithurae* (sensu Zhou et al., 2008) based on a synsacral count of 10, as basal ornithurines are characterized by synsacral counts of 9 (e.g., *Yixianornis*) or 10 (e.g., *Apsaravis*, *Baptornis*). Moreover, similar to *Apsaravis* (Clarke and Norell, 2002:fig. 10) and unlike many basal avialans, the midseries sacral vertebrae are subequal in length.

Micro-computed tomography of UA 9601 reveals the presence of distinct, transversely oriented, circumferential lumbosacral canals on the inner surface of the bony tube forming the synsacral canal (Fig. 2K). Similar to those known in extant birds, such canals (along with their associated soft tissues) are hypothesized to serve as a secondary balance-maintenance system, likely related to the unique form of bipedal locomotion observed in birds (see Necker, 1999, 2005, 2006, for a discussion of the neural and osteological correlates of the avian lumbosacral sensory system). This represents the first documentation of the lumbosacral sensory system in Mesozoic avialans, further underscoring the relatively derived nature of UA 9601. The microCT image also illustrates an enhanced degree of sacral enlargement of the spinal cord, as evidenced by the increased neural canal size in the mid-synsacral region (Fig. 2K).

These two synsacra clearly represent different avialan taxa (as noted above) and were recovered either within (UA 9601) or while trenching (FMNH PA 741) the block containing *Rahonavis ostromi*. Notably, neither specimen pertains to this taxon, be-

cause the holotype of *Rahonavis* (UA 8656) preserves a synsacrum with six fused vertebrae, each of which exhibit a relatively high (dorsoventrally) neural spine, quite unlike the restricted neural arches in both UA 9601 and FMNH PA 741.

**Coracoid**—One near-complete (FMNH PA 779) and one partial (UA 9602) coracoid have been recovered.

FMNH PA 779 is a nearly complete left coracoid from locality MAD 05-42. The strut-like coracoid was not fused to the scapula, as evidenced by a distinct, pit-like scapular cotyla (Fig. 3A, E). A procoracoid process is not present and the acrocoracoid process is straight, rather than medially directed (Fig. 3E). The acrocoracoid process bears a small articular facet for the furcula along its medial margin and a distinct longitudinal sulcus on its ventral surface (Fig. 3D). The glenoid facet is positioned ventral to the acrocoracoid process, at approximately the dorsoventral level of the scapular cotyla (Fig. 3C, E). The coracoid ramus is apneumatic with a straight lateral margin and no foramen or sulcus on the medial surface associated with the supracoracoideus nerve (Fig. 3D). There is, however, a small foramen positioned on the lateral surface of the ramus, approximately one-sixth of the distance from the cranial end (Fig. 3C). The sternal end is broad, with a modest lateral margin that does not exhibit a cranial projection (i.e., the lateral process of many authors). Although the medial margin of the sternal end is incompletely preserved, its dorsal surface is marked by a moderately well-developed fossa. This dorsal convexity at the sternal end is subdivided into two depressions by a longitudinal ridge (Fig. 3A), making it distinctive among the two preserved Maevarano coracoid morphologies (see below).

UA 9602 is another partial left coracoid (Fig. 3F–G) consisting of a caudal (sternal) articulation and associated ramus collected from locality MAD 93-18. Although the caudal and lateral margins of the sternal end are intact, the medial and dorsomedial edges are incomplete. A segment of the coracoid ramus was also collected; however, incomplete preservation of the edges precludes a direct association of it with the sternal end. Similar to FMNH PA 779, the coracoid ramus does not possess any features (e.g., procoracoid process, supracoracoid nerve foramen, etc.) typical of derived avialans. The cranial ('proximal' of Chiappe and Walker, 2002) end of the ramus is also incomplete (Fig. 3F); thus, it is not possible to assess the status of many potentially informative characters such as the shape of the acrocoracoid process or the position and shape of the glenoid facet.

The sternal articulation is extensive, with a distinct labrum on the caudodorsal margin (Fig. 3F–G). The labrum extends approximately four-fifths of the distance from the preserved medial edge. A distinct lateral margin is present; however, it does not exhibit a cranial or craniolateral projection, similar to the condition observed in FMNH PA 779. The element lacks the large fossa present in some basal birds (e.g., enantiornithines). Moreover, it does not exhibit the distinctive longitudinal ridge preserved in FMNH PA 779. UA 9602 was found in close proximity to the holotype (UA 8651) of *Vorona berivotrensis* at locality MAD 93-18, and although a direct association of the two specimens remains speculative, UA 9602 is size-consistent with a form such as *Vorona*.

Taken together, the two coracoids recovered from the Maevarano Formation preserve a mosaic of characteristics supporting a derived nonornithurine avialan or basal ornithurine referral. Significantly, key enantiornithine features (e.g., convex lateral margin of coracoid ramus, convex scapular articular facet) are not present, further restricting the referral. More specifically, the presence of a moderately developed lateral process and dorsally convex coracoid ramus suggest ornithurine affinities for FMNH PA 779 and UA 9602. However, the absence of a procoracoid process and a straight (rather than medially deviated) acrocoracoid process support a nonornithurine placement.

**Furculae**—FMNH PA 742 (Fig. 3H) and UA 9603 are partial furculae recovered from locality MAD 95-14. Although similar in gross morphology, not to mention being from opposite sides of the body, the specimens represent two individuals based on size differences and preserved morphologies.

FMNH PA 742 preserves the right ramus (including an unexpanded epicleidial process), symphysis, and a small portion (<10%) of the left ramus of a completely fused furcula (Fig. 3H). The furcular apophysis is represented only as a small, midline tubercle. The right ramus and symphysis are a craniocaudally (i.e., anteroposteriorly of Nesbitt et al., 2009) flattened, with the ramus oriented ~40 degrees from the midline (Fig. 3H). This allows for an estimated interclavicular angle of ~80 degrees. Using the perpendicular distance between the midline and the intact right terminus, the total width of the element was approximately 40 mm. The ventral margin of the symphysis appears gently curved (unlike the flat margin in certain ornithurines, e.g., *Yixianornis*; Clarke et al., 2006). Due to incomplete preservation, it is unclear if an extensive epicleidial process (*extremitas omalis clavicularae*; Baumel and Witmer, 1993) was present, although a fragmentary margin on the distal-most edge suggests at least some form of extension past the ventrally directed terminus. The coracoid (omal) end of the ramus has a small, caudally projecting hook originating from its medial edge (Fig. 3H), likely pertaining to the clavicular acromion process (see Baumel and Witmer, 1993). A distinct articular surface for the coracoid, as found in most birds, is not present. However, a very shallow depression near the terminal end may represent a contact for the coracoid (Fig. 3H).

UA 9603 is partial left furcula, similar in general morphology (e.g., a blunt terminus without a significantly expanded epiclei-

dial process) to FMNH PR 742. Notable differences between the two specimens include (1) a better-defined coracoid facet and (2) a ramus that is thicker medially than laterally (i.e., it does not possess a flat ramus as in FMNH PR 742) in UA 9603.

Pending the recovery of better preserved and/or articulated specimens, the two partial furculae are here tentatively referred to Ornithothoraces based on the flattened furcular ramus and estimated interclavicular angle of ~80 degrees in FMNH PA 742. Also, see Nesbitt et al. (2009) for a discussion of furcular morphology among theropods generally, and paravians specifically, as pertains to interclavicular angle assessments and ramus morphology.

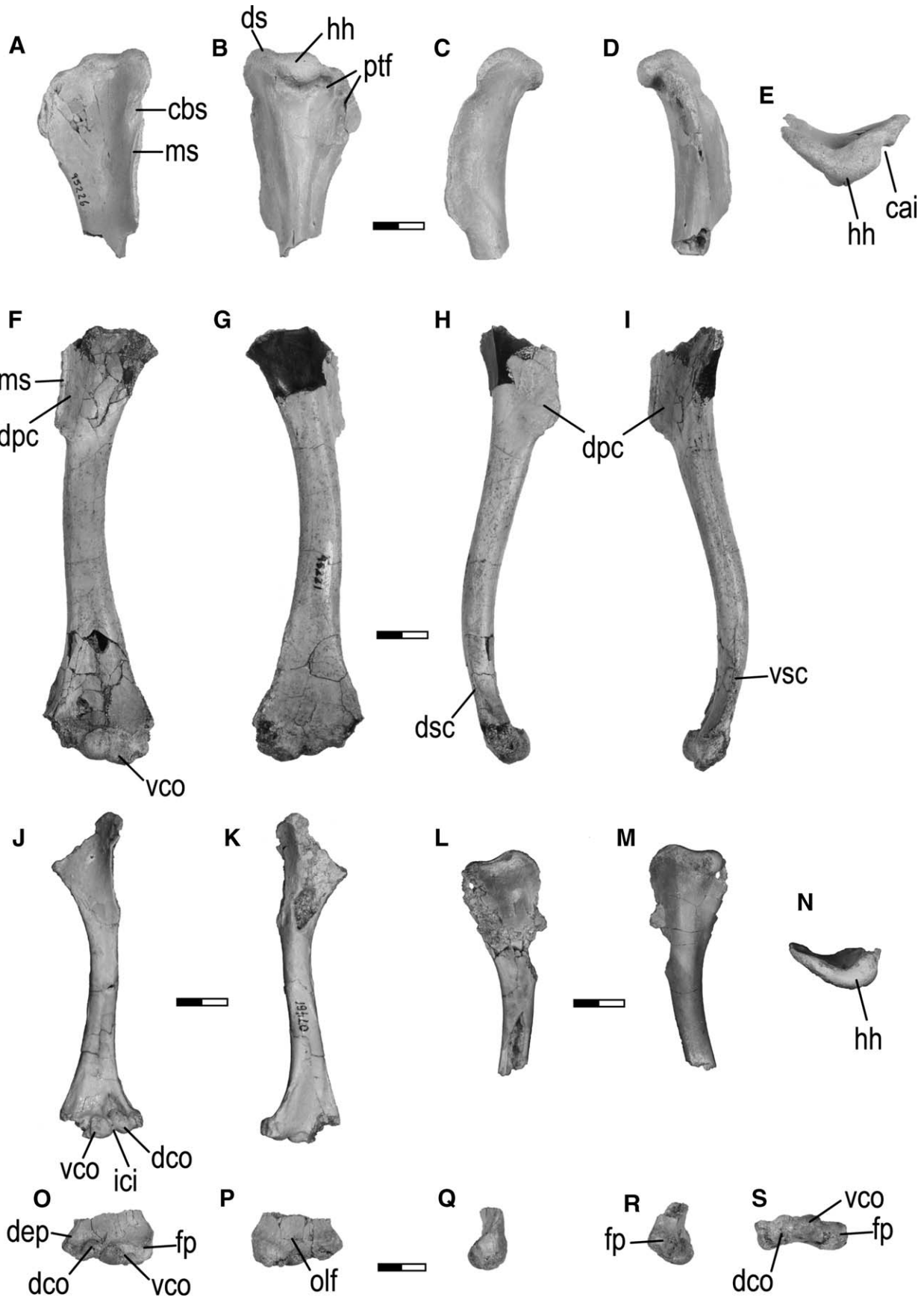
**Humeri**—Thirteen partial to complete humeri were recovered from locality MAD 93-18 between 1995 and 2005, and locality MAD 05-42 in 2007 (Figs. 4–8). Together these specimens provide the basis for establishing the wide range of body sizes (humeral midshaft diameter ranging from 1.3 to 9.5 mm) for the recovered avialans. Moreover, based on the presence of morphologically distinct humeri, it appears that at least six taxa of avialans were present in the Maevarano avifauna. However, because the isolated elements cannot be matched with confidence to either the other isolated elements (e.g., synsacra), or with other partial humeri (e.g., those represented by only proximal or distal ends), six represents a minimum number. The possible associations of some of these specimens with *Vorona berivotrensis* and *Rahonavis ostromi* are discussed below.

**Humeral Taxon A**—Three partial humeri (FMNH PA 743, FMNH PA 744, and FMNH PA 745) were collected from locality MAD 93-18. FMNH PA 743 is a partial left humerus (Fig. 4A–E) consisting of the proximal one-third of the element; the shaft is broken just distal to the distal end of the deltopectoral crest. FMNH PA 744 is a right humerus intact distally from approximately half way down the deltopectoral crest (Fig. 4F–I). The distal end of this element is variably preserved, with the dorsal condyle being mostly eroded. FMNH PA 745 is the distal articular end of a right humerus (Fig. 4O–S). Although slightly smaller in size (80% that of the larger specimen), the morphology of FMNH PA 745 is identical to that of FMNH PA 744.

Two additional humeri that are virtually identical in morphology to the above-mentioned specimens were collected from locality MAD 05-42. UA 9750 is a partial left humerus missing portions of the proximal and distal ends (Fig. 4J–K), and UA 9749 is the proximal half of a left humerus (Fig. 4L–N). Both represent individuals nearly identical in size to FMNH PA 745 (Fig. 4O–S), and thus, are approximately 80% the size of the two larger specimens of Humeral Taxon A (FMNH PA 743, FMNH PA 744).

FMNH PA 743 and FMNH PA 744, although proximal and distal humeri, respectively, possess enough overlap in the region of the distal deltopectoral crest to determine they are from the same taxon. For example, both possess a unique and distinctive, rugose ridge along the craniodorsal margin of a relatively straight deltopectoral crest. Moreover, comparable measurements from these (left- and right-sided) specimens demonstrate that they are nearly identical in size, from the same level in the quarry, and could derive from the same individual. Unfortunately, the lateral margin of the deltopectoral crest in the smaller UA 9749 and UA 9750 is not preserved. However, the preserved morphology of the proximal end of UA 9749 matches that of FMNH PA 743. FMNH PA 745 preserves only the distal-most articular portion of a right humerus, and matches FMNH PA 744 in specific morphology. The distal end of UA 9750 also matches that of FMNH PA 745 and FMNH PA 744. Thus, a composite based on these five specimens allows for a complete description of the entire humerus.

The well-defined, cranially convex humeral head is positioned in line with the main axis of the humeral shaft (i.e., it is centered on the proximal end; Fig. 4B). Whereas the humeral head is slightly bulbous, its profile still exhibits a slight cranial concavity and caudal convexity (Fig. 4E), thereby suggesting it belongs to



a nonornithurine avialan. Moreover, the head is dorsoventrally elongate and projects caudoventrally. The articular surface of the humeral head is confluent with the proximal surface of the dorsal 'shoulder,' which is notably narrower and distinct from the humeral head in proximal view (Fig. 4E). In cranial view a very shallow concavity is visible between the humeral head and dorsal shoulder, thereby resembling the condition in some enantiornithines (Walker et al., 2007). The humerus appears to lack a distinct dorsal tubercle, although there is some erosion along the proximodorsal margin of FMNH PA 743, and this area is missing in UA 9749. Nevertheless, the entire dorsal shoulder of the humerus extends proximally above the level of the humeral head (Fig. 4B). The proximoventral corner of the humerus (i.e., the location of the bicapital crest and ventral tubercle) is eroded in FMNH PA 743; what is preserved is a craniocaudally restricted projection, in contrast to the more blocky crests seen in some enantiornithines (e.g., PVL 4025). A deep but narrow sulcus is present on the cranial surface of the remaining bicapital crest and it is oriented roughly parallel to the deltopectoral crest (FMNH PA 743).

The ventral tubercle is not preserved on FMNH PA 743, although a distinct, rounded ridge extends dorsally and distally a short distance from its broken base. Distinct but shallow pneumotricipital fossae are located on either side of this ridge (Fig. 4B). The dorsal fossa is broader than the ventral and is situated adjacent to the ventrodorsal aspect of the humeral head and the distal margin of the capital groove. The capital groove is well separated from the inset dorsal margin of the pneumotricipital fossa and the two are not confluent. The caudal margin (margo caudalis), extending from the distal aspect of the humeral head, is broad and gently rounded.

The strong deltopectoral crest is short (~34% of humeral length), craniodorsally directed (as in *Patagopteryx*), and tapers abruptly at the distal end where it joins the humeral shaft (Fig. 4). Although the dorsal margin of the crest is slightly eroded, it appears to have been nearly straight. A raised, oval scar is positioned on the caudal surface of the crest, approximately two-thirds of the distance from its proximal edge (Fig. 4G). In cranial view the entire margin of the deltopectoral crest bears a strong raised muscle scar paralleling its dorsal margin (e.g., FMNH PA 743, FMNH PA 744).

The cranial surface of the proximal humerus is gently concave, with a slight depression just distal to the humeral head, in contrast to the deep depression observed in *Patagopteryx* and some enantiornithines (e.g., *Enantiornis*). A well-defined, raised, oval coracobrachialis scar is located immediately ventral to the inferred position of the dorsal tubercle near the proximal margin of the deltopectoral crest (also in *Enantiornis*). In dorsal view, the proximal humerus is cranially convex. Distal to the deltopectoral crest the humeral shaft exhibits slight craniocaudal compression. This trend continues distally such that the distal one-third of the humerus, including the condyles, is extremely craniocaudally compressed and approaches 60% of the midshaft thickness. The condyles exhibit a broad dorsoventral expansion, increasing in width to approximately 2.8 times that at humeral midshaft (Fig. 4F–G). The distal humerus exhibits a strong cranial deviation, imparting an apparent caudal convexity to the entire humeral shaft (Fig. 4H).

In cranial view, the bicondylar axis is canted slightly such that the ventral condyle extends further distally than the dorsal condyle (Fig. 4O). Although the distal humeral margin is not perpendicular to the long axis of the shaft, it lacks the strongly angled distal margin with the elongate flexor process observed in a number of avialans (e.g., enantiornithines such as *Cathayornis*, *Penegornis* [Zhou et al., 2008], *Apsaravis* [Clarke and Norell, 2001], Humeral Taxon C, FMNH PA 748, UA 9607). The cranially projecting ventral condyle is bulbous and nearly hemispherical in distal view (Fig. 4S). It is well inset from the large, squared off and pronounced ventral epicondyle and blocky flexor process. The cranial surface of the ventral epicondyle/flexor process, immediately ventral to the ventral condyle, bears two distinct fossae (Fig. 4O): a third fossa, the ventrodorsal fossa, is located on the ventral aspect of the ventral epicondyle (Fig. 4S). A distinct muscle scar extends proximally along the ventral margin of the shaft (approximately one-fourth of the distance from the distal end) from the ventrodorsal fossa. A distinct ventral supracondylar tubercle is not present.

The bulbous dorsal condyle is slightly smaller than its ventral counterpart. This condyle wraps caudodorsally around the distal margin of the humerus and appears elongate and obliquely oriented in distal view (Fig. 4S). A narrow, shallow, oblique intercondylar groove separates the ventral and dorsal condyles. A distinct brachialis fossa is located on the cranial surface of the humerus just proximal to the dorsal condyle (Fig. 4J). This fossa is short and sub-circular in FMNH PA 744 and FMNH PA 745, and slightly deeper and more proximodistally elongate in UA 9750. A distinct brachialis fossa is found in more derived ornithurines (e.g., *Ichthyornis*, *Limenavis*, *Lithornis*; Clarke and Chiappe, 2001), although one may also be present in the enantiornithine *Neuquenornis* (Chiappe and Calvo, 1994; Clarke and Chiappe, 2001). There is a moderately developed dorsal epicondyle that bears a large irregular fossa on its dorsal surface (Fig. 4H, Q). A short, thin lamina extends proximally from the dorsal margin of the dorsal epicondyle and similar to the ventral humeral margin, bears a raised, rugose scar along its crest (Fig. 4F–H). This muscle scar is approximately one-third the length of the corresponding feature on the ventrodorsal humerus. An elongate, well-demarcated fossa occurs along the cranial margin of this lamina, proximal to the dorsal epicondyle. This lamina and fossa corresponds in location and orientation to the dorsal supracondylar tubercle of ornithurines (e.g., *Limenavis*, *Ichthyornis*; Clarke and Chiappe, 2001) and the attachment point for *m. extensor carpi radialis*.

The caudal surface of the distal humerus exhibits a small, poorly defined olecranon fossa that is restricted to the area immediately proximal to the ventral condyle and intercondylar groove (Fig. 4G, P). The remaining surface of the caudodistal humerus is gently concave and generally nondescript, lacking both humerotricipital and scapulotricipital sulci.

Based on the mosaic of characters preserved in this large and relatively robust taxon, we determine that it is likely from a nonornithurine form, yet its exact placement among ornithothoracines is problematic. For example, whereas some features (e.g., proximally positioned deltopectoral crest and dorsal shoulder; see PVL 4022 in Chiappe and Walker, 2004) suggest enantiornithine affinities, other features do not (e.g., the distal end is

← FIGURE 4. Partial avialan humeri of 'Humeral Taxon A' (?*Vorona berivotrensis*). Proximal left humerus (FMNH PA 743) in cranial (A), caudal (B), dorsal (C), ventral (D), and proximal (E) views. Partial right humerus (FMNH PA 744) in cranial (F), caudal (G), dorsal (H), and ventral (I) views. Partial left humerus (UA 9750) in cranial (J) and caudal (K) views. Proximal right humerus (UA 9749) in cranial (L), caudal (M), and proximal (N) views. Distal end of right humerus (FMNH PA 745) in cranial (O), caudal (P), dorsal (Q), ventral (R), and distal (S) views. Cranial is toward the top of the page in E, N, and S. **Abbreviations:** *cai*, capital incisure; *cbs*, coracobrachialis scar; *dco*, dorsal condyle; *dep*, dorsal epicondyle; *dpc*, deltopectoral crest; *ds*, dorsal shoulder; *dsc*, dorsal supracondylar crest; *fp*, flexor process; *hh*, humeral head; *ici*, intercondylar incisure; *ms*, muscle scar; *olf*, olecranon fossa; *ptf*, pneumotricipital fossa; *vco*, ventral condyle; *vsc*, ventral supracondylar crest. Scale bars equal 1.0 cm.

not significantly expanded or slanted relative to the humeral shaft, etc.). The size of the two larger elements (FMNH PA 734, FMNH PA 744) corresponds well to that of the known hind limb elements of *Vorona berivotrensis*. Moreover, the preserved morphology is consistent with a hypothesized phylogenetic position among relatively derived non-ornithurine Avialae. Given the size-similarity and composite morphology of the five specimens, we tentatively refer Humeral Taxon A to *Vorona*. However, until articulated/associated materials are recovered this referral remains an untested hypothesis.

There are two size classes represented in Humeral Taxon A. One size class is represented by the identically sized FMNH PA 743 and FMNH PA 744; the other class by the three specimens (FMNH PA 745, UA 9749, UA 9750) that are approximately 80% the size of the larger specimens. Thus, it is not known whether these size differences relate to ontogenetic staging, sexual dimorphism, or even species differences that are not manifest in the preserved morphologies (also see the section on ulnae below).

**Humeral Taxon B**—FMNH PA 746 and UA 9604 are identically sized distal left and right humeri (Fig. 5) collected from locality MAD 93-18. The humeral shaft is craniocaudally compressed to 70% its width and is gently convex caudally. The distal end flares to approximately 2.3 times the width of the midshaft and the bicondylar axis is canted such that the ventral condyle extends further distally than the dorsal condyle (Fig. 5A, F). The ventral and dorsal condyles are large and bulbous in both cranial and distal views (Fig. 5E, J), and together occupy nearly the entire width of the distal end. In distal view the ventral condyle is approximately 25% narrower craniocaudally than the dorsal condyle (Fig. 5J). The intercondylar incisure is very shallow and oriented craniocaudally (Fig. 5J), rather than obliquely as in most avialans. The ventral epicondyle is moderately developed, craniocaudally expanded, and gently rounded around its ventral margin (Fig. 5D, F, I). The dorsal epicondyle is only very weakly developed. There is a well-developed, blunt flexor process projecting distally past the ventral condyle.

The cranial (flexor) surface of the distal humerus is slightly concave and nearly featureless, lacking a distinct brachialis fossa (Fig. 5A). Caudodistally there is a small, shallow, crescentic olecranon fossa just proximal to the ventral condyle and intercondylar sulcus (Fig. 5G). The general morphology exhibited by FMNH PA 746 and UA 9604 is relatively simple, and similar to that observed in the much smaller FMNH PA 747 (Humeral Taxon C; see below).

The two known specimens of this taxon represent left and right sides of identical sized elements, and may pertain to the same individual. Both were discovered in close proximity to the *Rahonavis ostromi* holotype (UA 8656) in the same year and in same level of quarry MAD 93-18. Significantly, these specimens are size consistent with the ulna of *Rahonavis* (the right ulna was described by Forster et al., 1998). Perhaps more importantly, the distal right humerus described here (UA 9604) articulates perfectly with the right ulna of *Rahonavis*. FMNH PA 746 was recovered approximately 1.0 m west of *Rahonavis*; UA 9604 was collected with miscellaneous quarry specimens and its exact location was not recorded. However, based on both the field notes and quarry numbers, it was collected in the same end of the quarry as *Rahonavis*.

In summary, four lines of evidence support a tentative referral of FMNH PA 746 and UA 9604 to *Rahonavis*, the strongest two represented by size consistency and anatomical congruence of humeral and ulnar articular surfaces. Third, the provenance of the individual specimens within the quarry minimally places the elements in proximity to one another. Finally, the two humeri represent a taxon with morphology (e.g., craniocaudally oriented intercondylar incisure) characteristic of basal forms exhibiting a mosaic of avialan and nonavialan theropod features, similar to that preserved in the holotype of *Rahonavis*.

**Humeral Taxon C**—FMNH PA 747 is a small, nearly complete right humerus (Fig. 6A–F) recovered from MAD 93-18. It was found within the *Rahonavis ostromi* jacket during preparation, but, due to its size and overall morphology, is from a different and far smaller individual and taxon.

The humeral head is nearly indistinct from the thick dorsal shoulder of the humerus, with the two together forming a dorsoventrally elongate proximal articular end (Fig. 6E). This differs from the situation in Humeral Taxon A, where the bulbous humeral head is easily distinguishable from the narrow dorsal articular margin, but is similar to other primitive avialans and most enantiornithine birds (e.g., *Gobipteryx*; also see Zhou et al., 2008). Ventral to the humeral head is a prominent and well-defined ventral tubercle that is directed caudoventrally (Fig. 6D, E). A shallow pneumotricipital fossa is positioned between the ventral tubercle and humeral head, and a distinct capital groove is present (Fig. 6B, E), as in most enantiornithines (e.g., *Concornis*; Sanz et al., 1995) and more derived avialans (e.g., *Apsaravis*; Clarke and Norell, 2001). The bicipital crest is modestly developed (Fig. 6D). The cranial surface of the bicipital crest is damaged and no additional morphology can be observed. The deltopectoral crest is very short (30% total length of humerus) and tapers abruptly at the distal end. Its width approximates that of the humeral shaft. The dorsal margin of the deltopectoral crest is thin, slightly convex, and directed dorsally (Fig. 6A). A dorsal tubercle is not present, although some damage to the proximodorsal margin may obscure its presence. Despite some damage and crushing on the cranial surface, the proximal margin of a depression can be seen just distal to the humeral head (Fig. 6A). The area of the coracobrachialis scar is crushed and poorly preserved, obscuring its presence or absence.

The long, gracile humeral shaft is caudally convex (Fig. 6C). The humeral diaphysis is craniocaudally compressed, a condition that is accentuated at the distal condyles. The condyles are approximately 2.7 times the width of the midshaft diameter and the bicondylar axis is angled, with the ventral condyle extending further distally (Fig. 6A). This offset is further accentuated by the presence of a well-developed, blunt flexor process extending distally from the ventral condyle. The dorsal and ventral condyles are both elongate, subequal in width, span nearly the entire distal end, and are separated from one another by a narrow, shallow craniocaudally oriented intercondylar incisure (Fig. 6F). The ventral condyle is slightly larger than the dorsal in cranial view, although craniocaudally narrower in distal view. The cranial face of the expanded distal end is slightly concave and lacks a distinct brachialis fossa (Fig. 6A). There is a well-developed, craniocaudally blocky and ventrally rounded ventral epicondyle, and a moderately developed dorsal epicondyle. On the caudal surface of the distal end there is a shallow, crescentic olecranon fossa just proximal to the ventral condyle and intercondylar groove (Fig. 6B).

Humeral Taxon C is here referred to enantiornithines based on the following features: a strongly bowed shaft, proximally positioned deltopectoral crest and dorsal shoulder, and distal paracondylar expansion (Chiappe and Walker, 2002). And although clearly different in size, the overall morphology of the distal end of FMNH PA 747 is quite similar to that of Humeral Taxon B. The two forms are distinguishable in that Humeral Taxon C exhibits a distinct dorsal epicondyle whereas Humeral Taxon B does not.

**Humeral Taxon D**—UA 9605 is a proximal left humerus, broken at midshaft and missing its distal end (Fig. 6G–K), recovered from locality MAD 93-18. UA 9605 is approximately 14% larger than FMNH PA 747 (Humeral Taxon C; Fig. 6A–F). Although similar to FMNH PA 747 in many aspects (e.g., a humeral head that is indistinct from a craniocaudally expanded dorsal shoulder), it also exhibits a number of distinctive features. For example, the humeral head is craniocaudally restricted relative to the dorsal shoulder in UA 9605 (Fig. 6K). Although

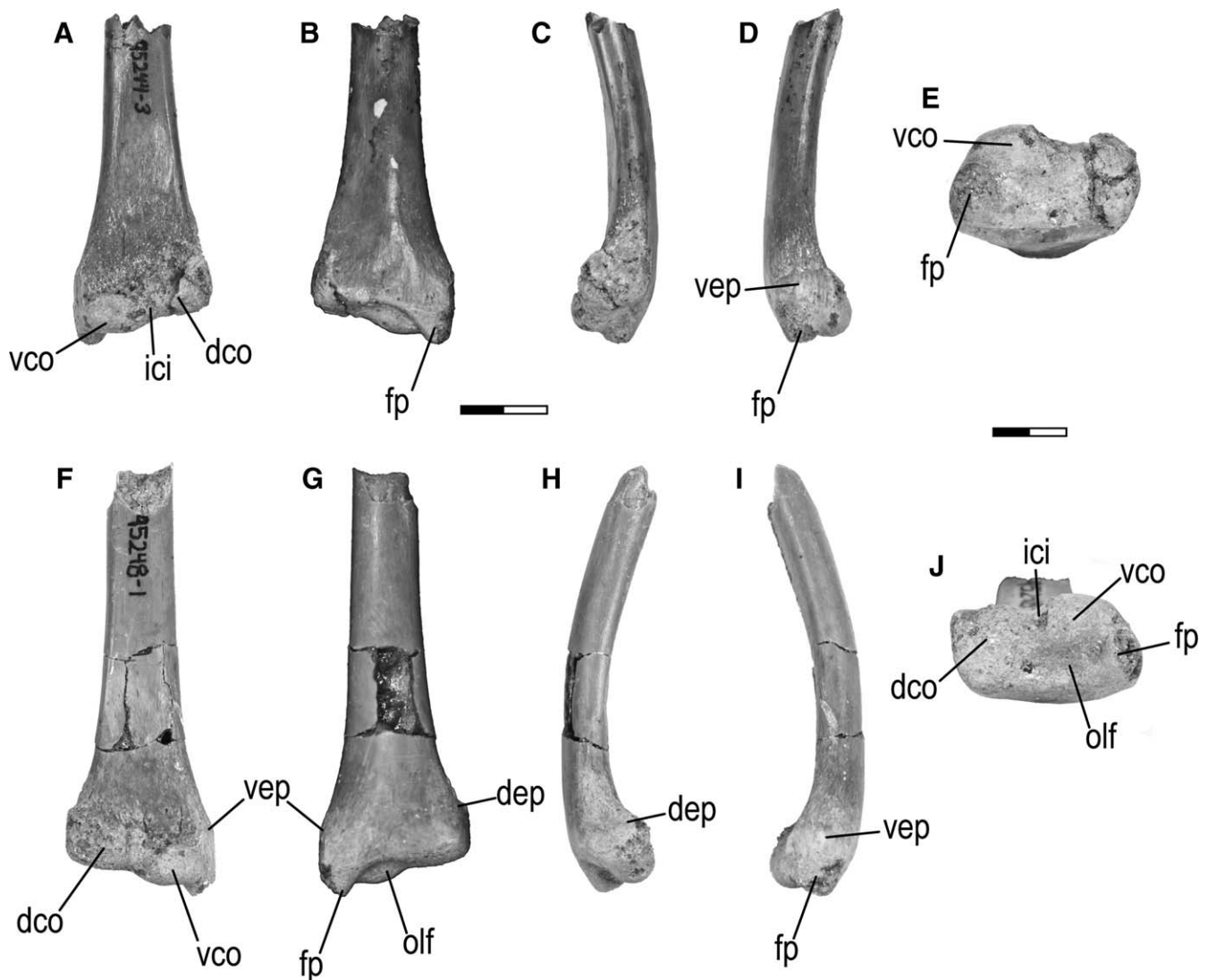


FIGURE 5. Partial avialan humeri of 'Humeral Taxon B' (?*Rahonavis ostromi*). Distal left humerus (FMNH PA 746) in cranial (A), caudal (B), dorsal (C), ventral (D), and distal (E) views. Distal right humerus (UA 9604) in cranial (F), caudal (G), dorsal (H), ventral (I), and distal (J) views. Cranial is toward the top of the page in E and J. **Abbreviations:** dco, dorsal condyle; dep, dorsal epicondyle; fp, flexor process; ici, intercondylar incisure; olf, olecranon fossa; vco, ventral condyle; vep, ventral epicondyle. Scale bar equals 1.0 cm in A–D and F–I and 0.5 cm in E and J.

much of the ventral tubercle is broken, the remaining portion suggests it was well developed. The crus of the ventral tubercle is sharp and well defined in UA 9605 (Fig. 6H), unlike the more rounded strut observed in FMNH PA 747 (Humeral Taxon C). The ventral tubercle and humeral head are separated by a well-defined capital incisure and a very shallow and narrow pneumotricipital fossa, characters consistent with most enantiornithines and some more-derived avialans (Zhou et al., 2008). Only the proximal-most portion of the bicipital crest is present, where it was craniocaudally thickened immediately ventral to the base of the ventral tubercle (Fig. 6J). The ventral margin of the bicipital crest parallels the humeral shaft.

The deltopectoral crest projects dorsally (Fig. 6H, I). As the dorsal margin of the crest is incomplete, it is impossible to ascertain its entire shape, inclination, and width. However, it appears that the distal margin of the deltopectoral crest slopes to join the humeral shaft at a low angle (Fig. 6H), in contrast to the abrupt, high-angle transition in forms such as in FMNH PA 747 (Humeral Taxon C; Fig. 6B). The cranial surface of the proxi-

mal humerus preserves a well-developed oval fossa just distal to the humeral head (Fig. 6G), similar to that observed in enantiornithines (e.g., PVL 4025) and other basal avialans. However, the proximodistal extent of the fossa in UA 9605 is quite restricted when compared to these other forms (e.g., see *Martinavis*; Walker et al., 2007). There is a slightly eroded, oval coracobrachialis muscle scar, and the cranial surface of the dorsal deltopectoral crest margin appears slightly roughened.

**Humeral Taxon E**—UA 9606 is an extremely fragmentary right humerus (Fig. 6L–M) recovered from locality MAD 93-18. The specimen is missing the proximal end and everything distal to the termination of the deltopectoral crest. However, the specimen is significant in that it preserves on its cranial surface a large, oval coracobrachialis scar just distal to the dorsal shoulder and a shallow, longitudinal groove paralleling the dorsal margin of the deltopectoral crest (Fig. 6L). In these features it is very similar to Humeral Taxon A (e.g., FMNH PA 743; Fig. 4A). In contrast to Humeral Taxon A, however, the cranial surface of UA 9606 is nearly flat (versus a notably concave condition in the

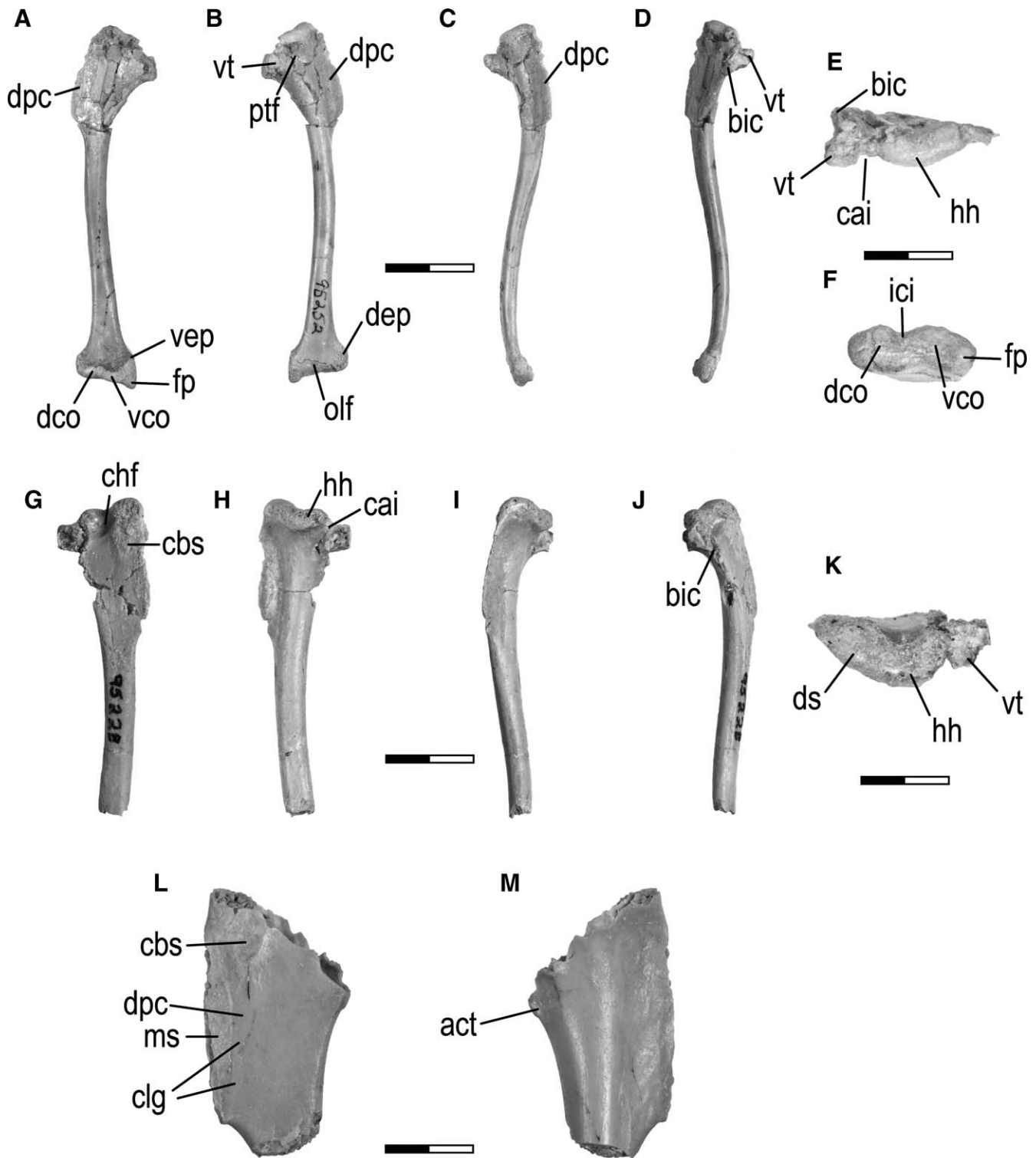


FIGURE 6. Humeri of medium-sized Avialae (?Enantiornithes) indet. Complete right humerus of ‘Humeral Taxon C’ (FMNH PA 747) in cranial (A), caudal (B), dorsal (C), ventral (D), proximal (E) and distal (F) views. Partial left humerus of ‘Humeral Taxon D’ (UA 9605) in cranial (G), caudal (H), dorsal (I), ventral (J), and proximal (K) views. Partial right humerus of ‘Humeral Taxon E’ (UA 9606) in cranial (L) and caudal (M) views. Cranial is toward the top of the page in E, F, and K. **Abbreviations:** act, accessory tubercle; bic, bicipital crest; cai, capital incisure; cbs, coracobrachialis scar; chf, caudal humeral fossa; clg, caudal longitudinal groove; dco, dorsal condyle; dep, dorsal epicondyle; dpc, deltopectoral crest; ds, dorsal shoulder; fp, flexor process; hh, humeral head; ici, intercondylar incisure; ms, muscle scar; olf, olecranon fossa; ptf, pneumotricipital fossa; vco, ventral condyle; vep, ventral epicondyle; vt, ventral tubercle. Scale bar equals 1.0 cm in A–D and G–J, and 0.5 cm in E–F, K, and L–M.

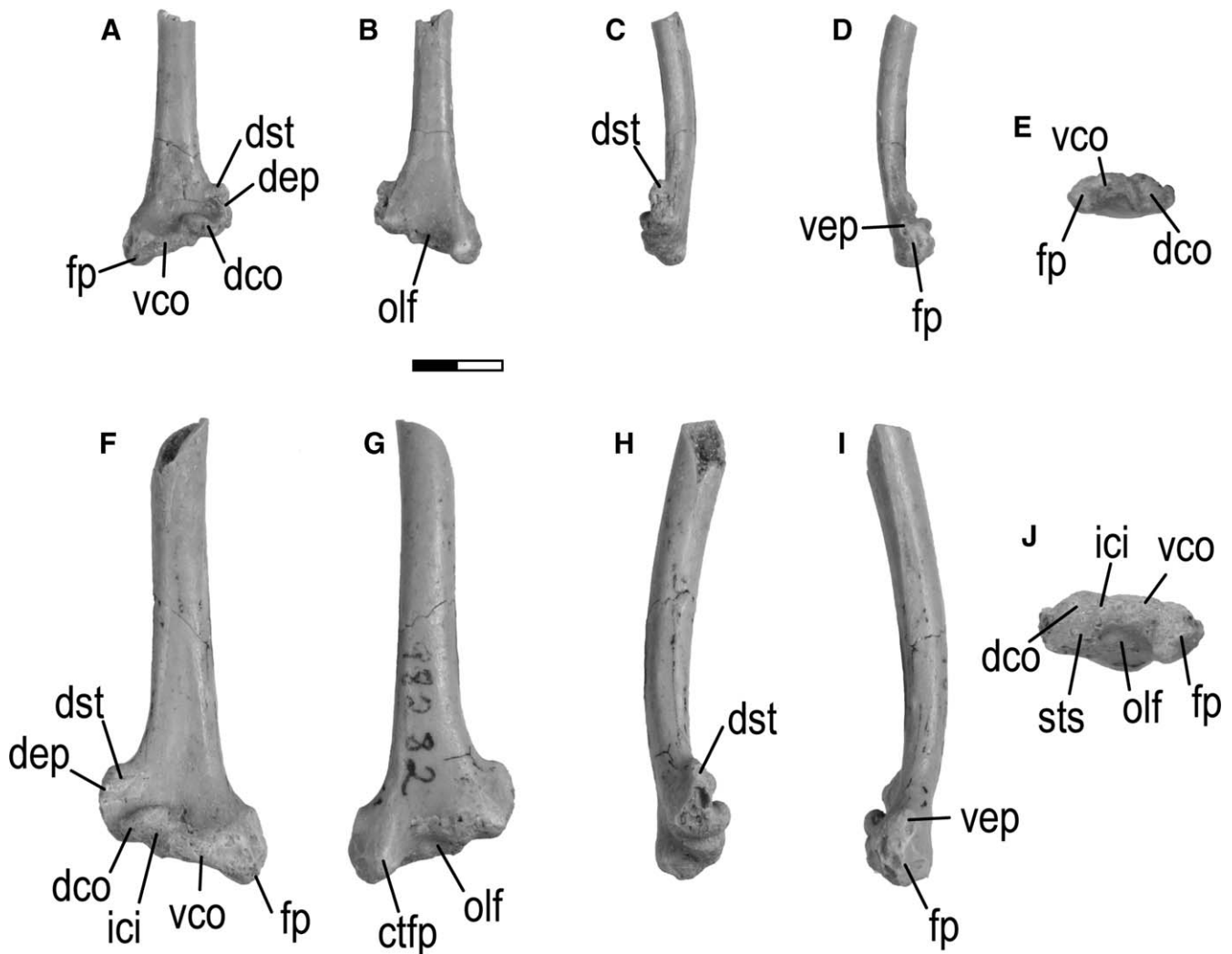


FIGURE 7. Humeri of small-sized Avialae (?Ornithurae) indet. Distal left humerus (FMNH PA 748) in cranial (A), caudal (B), dorsal (C), ventral (D), and distal (E) views. Distal right humerus (UA 9607) in cranial (F), caudal (G), dorsal (H), ventral (I), and distal (J) views. Cranial is toward the top of the page in E and J. **Abbreviations:** ctfp, caudal tubercle of flexor process; dco, dorsal condyle; dep, dorsal epicondyle; dst, dorsal supracondylar tubercle; fp, flexor process; ici, intercondylar incisure; olf, olecranon fossa; sts, scapulotricipital sulcus; vco, ventral condyle; vep, ventral epicondyle. Scale bars equal 0.5 cm.

former), and the longitudinal groove along the deltopectoral crest is relatively much wider (Fig. 6L) than in Humeral Taxon A. The deltopectoral crest is eroded along its entire dorsal margin, but the preserved portion projects dorsally, and appears to have had an abrupt transition to the humeral shaft. A small, but distinct tubercle is present on the caudoventral surface of the proximal humerus (Fig. 6M), just distal to the break (and just distal to the location of the bicipital crest). This morphology is unique among all the Maevarano avialans.

**Humeral Taxon Unknown**—FMNH PA 748 and UA 9607 are represented by small, isolated distal humeri (Fig. 7), both of which were recovered from locality MAD 93-18. Based on both morphological and size criteria, these two specimens clearly differ from Humeral Taxa A, B, and C described above. However, because Humeral Taxa D and E are based on specimens lacking distal ends, and these two taxa are generally size consistent with both FMNH PA 748 and UA 9607, there is no way to definitely associate or refute an association of these two latter specimens with either Humeral Taxa D or E. FMNH PA 748 is a distal left humerus (Fig. 7A–E) and UA 9607 is a distal right humerus (Fig.

7F–J), and although the former is only 65% the size of the latter, they are virtually identical and are described together here.

The humeral shaft is craniocaudally compressed and caudally convex. The distal end is dorsoventrally expanded to approximately 3.2 times the width at midshaft (Fig. 7A, F), a feature found in many enantiornithines (e.g., PVL 4025). The distal end is strongly canted such that the ventral condyle is distally positioned relative to the dorsal condyle. Moreover, a distinct, blunt flexor process is present on the ventrodistal end of the element. A prominent tubercle is present on the caudal surface of the flexor process, similar to that observed in derived enantiornithines (Chiappe and Walker, 2002). In cranial view, the ventral condyle is dorsoventrally elongate and angled distally toward the flexor process (Fig. 7A, F). The more prominent and bulbous dorsal condyle is elongate and more proximally located. However, it is oriented opposite that of the ventral condyle. The two condyles are separated by a moderately well-defined, obliquely oriented intercondylar incisure that wraps caudodorsally around the distal end, paralleling the long axis of the elongate dorsal condyle (Fig. 7A, F, J).

The flexor process and ventral epicondyle are both well developed and craniocaudally expanded (Fig. 7D, I). The blocky flexor process projects below the level of the ventral condyle, but lacks the elongate blunted tip seen in some basal avialans. The cranial and ventral surfaces of the ventral epicondyle are pitted by at least seven distinct confluent fossae. In addition, a single fossa is located on the cranial surface of the distal flexor process. Similar fossae are also found in some enantiornithines (e.g., PVL 4025) and ornithurines (e.g., *Limenavis*; Clarke and Chiappe, 2001).

The dorsal epicondyle is extremely well developed and a dorsal supracondylar tubercle is present just proximal to its craniodorsal margin (Fig. 7F, H). On the cranial surface, the dorsal supracondylar tubercle is separated from the dorsal condyle by a deep, obliquely oriented groove that is confluent with the shallow brachialis fossa. The terminus of the dorsal supracondylar tubercle bears a circular fossa that is directed craniodorsally. This morphology is known in *Ichthyornis* and more derived ornithurine birds (Clarke and Chiappe, 2001; Zhou et al., 2008), and may be present in some nonornithurine avialans (e.g., *Cathayornis*, *Patagopteryx*; Zhou et al., 2008).

On the caudal surface there is a moderately deep and well-defined olecranon fossa (Fig. 7B, G). The intercondylar incisure does not enter the olecranon fossa in FMNH PA 748 or UA 9607, but is separated from it by a slight ridge. This ridge also demarcates a slightly depressed area dorsal to the olecranon fossa that may represent an incipient scapulotricipital sulcus (Fig. 7J), a morphology known only in derived ornithurines (e.g., *Ichthyornis*, crown-clade Aves). The well-defined ventral margin of the olecranon fossa is formed by a caudally projecting tubercle that lies on the caudal surface of the flexor process (Fig. 7G). Taken together, a well-defined dorsal supracondylar tubercle, an incipient scapulotricipital sulcus, and the assortment of small fossae on the distal end (e.g., fossae associated with the ventral epicondyle) suggest ornithurine affinities for the two specimens.

**Humeral Taxon F**—FMNH PA 749 is a very small, partial left humerus (Fig. 8A–D) preserving a 16.5-mm segment from the distal-most deltopectoral crest to the condyles; it was recovered from locality MAD 93-18. The distal condyles are craniocaudally compressed; however, due to breakage and erosion, all specific condylar morphology is obscured. From the gross proportions that are present, it appears that the distal end of the humerus was dorsoventrally expanded to at least 3 times that of the mid-shaft; this is a conservative estimate because the distal end of the element is incomplete. The distal expansion appears gradual and nearly equal in dorsal and ventral directions. In this regard FMNH PA 749 is similar to that of Humeral Taxon A (Fig. 4), but different from that of Humeral Taxa B, C, and Unknown(s) (see above). Despite the deformed and missing ends, such broadly flaring condyles are reminiscent of those known in most enantiornithines. In dorsal view, the shaft is caudally convex. Although only the distal end of the deltopectoral crest is present, it appears to be oriented craniodorsally and at about 45 degrees relative to the long axis of the distal condyles (Fig. 8). Given the lack of detailed morphology of the proximal and distal ends of FMNH PA 749, we are reluctant to assign Humeral Taxon F to any known groups, and simply refer it to Avialae indeterminate at present. It is notable, however, in its extremely small size (estimated total length of 19 mm) relative to most known Mesozoic avialans.

**Ulnae**—Three partial to complete ulna have been recovered. Two of these (FMNH PA 750 and UA 9751) differ in size but are otherwise identical in morphology. The third specimen (UA 9608), preserving only the proximal end, is nevertheless distinct from the other two specimens.

FMNH PA 750, recovered from locality MAD 93-18, is a crushed left ulna preserving the shaft and part of the distal end. Although incomplete proximally, the preserved length of FMNH PA 750 is 129 mm with a dorsoventral midshaft diameter of 6.2 mm (Fig. 9F).

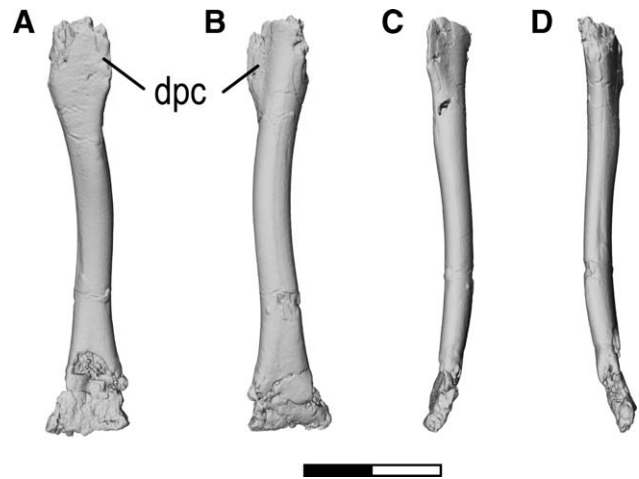


FIGURE 8. Humerus of very small Avialae indet. Left humerus (FMNH PA 749) of ‘Humeral Taxon F’ in cranial (A), caudal (B), dorsal (C), and ventral (D) views. **Abbreviations:** dpc, deltopectoral crest. Scale bars equal 0.5 cm.

The incomplete proximal end preserves the flaring bases of the dorsal and ventral cotyles, and the distal-most impression of a shallow, slightly roughened fossa that likely represents the radial incisure (Fig. 9F). The margins of the fossa join distally and continue down the shaft as a weakly developed interosseous ridge. A small foramen is located along this ridge, just distal to the radial incisure.

The ulnar shaft has a slight S-shaped curvature. The shaft is notably flattened along the entire dorsal surface, but rounded on other aspects. The caudal margin is narrow and shows no evidence of remigial papillae. Although the distal end of the ulna is slightly crushed, it appears as though it is dorsoventrally compressed (Fig. 9F). The margins of the condyles are eroded, particularly so of the dorsal condyle and no other definitive condylar morphology is apparent. Although a direct association is not possible, FMNH PA 750 is size-consistent with a taxon the size of *Vorona*.

UA 9751 is a complete left ulna (Fig. 9A–E) from locality MAD 05-42. Although only 72% the size of FMNH PA 750, it is otherwise virtually identical, including the general curvature profile, a flattened surface on the dorsal aspect of the shaft, and characteristic dorsoventral compression of the distal end. Although the distal end is more complete and less crushed than in FMNH PA 750, UA 9751 does not preserve the extreme distal or dorsal margins of the condylar end. The preserved morphology of the distal end is nearly featureless and lacks a clear separation between the dorsal and ventral condyles (Fig. 9C–D). One notable feature is the proximodistally oriented tendinous incisure located on the dorsal aspect of the distal end (Fig. 9C).

The proximal end of UA 9751 is nearly complete (Fig. 9E). Similar to FMNH PA 750 it exhibits a shallow fossa for the radial incisure, although the fossa is only faintly visible on the smaller specimen. As in FMNH PA 750, the distal end of the radial incisure marks the beginning of a faint interosseous line that is perforated by a small nutrient foramen in a similar location (Fig. 9D). The dorsal cotyle projects prominently from the cranial margin of the shaft and is dorsoventrally compressed. The articular surface of the dorsal cotyle slopes ventrally and is very slightly convex (Fig. 9E). The ventral cotyle and olecranon process are eroded and incomplete. However, the articular surface of the ventral cotyle appears to have also been steeply canted ventrally, and craniocaudally broad. There is no apparent intercotylar crest.

There is a roughened area of bone at the position of the brachialis fossa (Fig. 9D), but without any definitive depression associated with it.

As with Humeral Taxon A, we cannot determine at this time whether the size difference between FMNH PA 750 and UA 9751 is due to ontogeny, dimorphism, or taxonomic differences not manifest in the preserved ulnar morphologies.

UA 9608 is the proximal end of a right ulna recovered from locality MAD 93-18. The olecranon process is fairly well developed, projecting proximally past the level of the ventral cotyle (Fig. 9I). The margin of the dorsal cotyle is eroded, thus its complete shape and size cannot be determined. The small portion that is preserved exhibits a slightly convex articular surface. The articular surface of the ventral cotyle is concave. The two cotylar surfaces are separated by a weak intercotylar incisure (Fig. 9I). A longitudinal muscular ridge passes distally from the well-defined distal edge of the ventral cotyle. The brachialis fossa is represented by a small, sub-circular depression positioned just distal to the ventral cotyle. A convex dorsal cotyle separated from a concave ventral cotyle by a distinct intercotylar incisure is characteristic of certain enantiornithines (e.g., see *Concornis*; Sanz et al., 1995).

**Radius**—FMNH PA 751 is poorly preserved proximal (right?) radius (Fig. 9K–L) recovered from locality MAD 93-35. Although poorly preserved, the specimen consists of the radial head and proximal portion of the diaphysis. The radial head is cranio-caudally compressed (Fig. 9L) and a proximodistally elongate bicipital tubercle is located approximately 2 mm from the proximal end. The radial diaphysis is oval in cross-section.

**Carpometacarpus**—FMNH PA 780 is a near-complete left carpometacarpus recovered from locality MAD 05-42. There are no phalanges or proximal carpals associated with the specimen.

The carpometacarpus is 23.2 mm in length. Whereas the semilunate carpal and proximal ends of the metacarpals are completely fused to one another, the major and minor metacarpals are not fused distally (Fig. 9O). Moreover, the minor metacarpal exceeds the major metacarpal in length by ~2.0 mm. Taken together, these features are similar to those identified in enantiornithines (e.g., *Enantiornis*; Chiappe and Walker, 2002; *Pengornis*; Zhou et al., 2008).

Proximally, the carpal trochlea is dorsoventrally compressed. The dorsal and ventral margins of the trochlea are separated from one another by a modest ginglymus (Fig. 9Q). The dorsal margin is slightly wider and extends further proximally than its ventral counterpart. In dorsal view, the trochlea subscribes a nearly hemispherical arch that is positioned over the proximal ends of the major and minor metacarpal (Fig. 9O), so that the trochlea lies caudal to the alular metacarpal. There is a very shallow and poorly defined caudal carpal fovea, and a moderately well circumscribed cranial carpal fovea (Fig. 9M).

A very well developed, dorsoventrally compressed extensor process projects cranially from the base of the carpal trochlea. The distal margin of this process is square in dorsal view, contrasting with the very rounded margin of the extensor process present in *Neuquenornis* (Chiappe and Calvo, 1994). Due to incomplete preservation, it is difficult to discern if a separate alular process was present; minimally, the craniodistal corner of the extensor process is dorsoventrally expanded into a rounded, non-ginglymoid cotyle that presumably articulated with the first alular phalanx.

Immediately caudal to the extensor process on the ventral aspect is a deep and well-defined fossa that occupies the entire proximal end of the major metacarpal. This fossa is oval in outline, with the long axis oriented proximodistally. A small, cranially projecting pisiform process slightly overhangs the caudal margin of the fossa (Fig. 9P). The area of the infratrochlear fossa is slightly concave and poorly defined.

The shaft of the major metacarpal is straight and fairly uniform in diameter throughout its length (Fig. 9P). The shaft of the minor

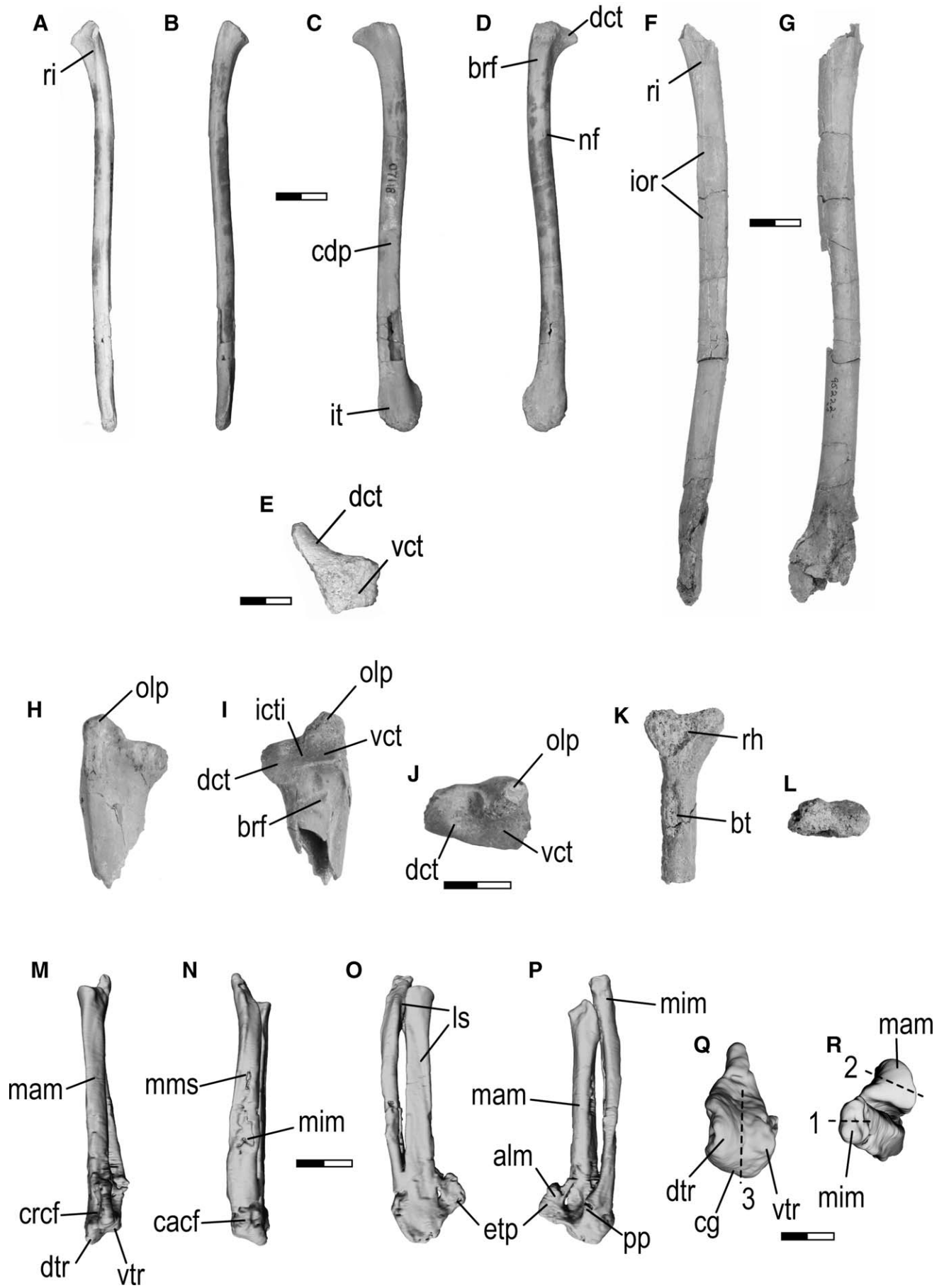
metacarpal is slightly convex caudally; distally it broadens cranio-caudally while narrowing dorsoventrally (Fig. 9R). The cranio-caudal width (at midshaft) of the minor metacarpal is approximately 60% of that of the major metacarpal; just proximal to the distal condyles it expands to approximately 70% of the major metacarpal (Fig. 9O–P). By contrast, the dorsoventral extent of the minor metacarpal exceeds that of the major metacarpal proximally, and although narrowing distally, it still slightly exceeds the major metacarpal in depth at midshaft. Distal to midshaft the major metacarpal exceeds that of the minor in all dimensions.

There is no development of an intermetacarpal process or tubercle. The dorsal surface of the major metacarpal is flattened and incised by a well-defined ligament sulcus that extends obliquely from the cranioproximal to caudodistal margins. The sulcus continues onto the cranial surface of the distal end of the minor metacarpal, where it occupies a position in between the opposed, unfused ends of the major and minor metacarpals (Fig. 9O). A broad sulcus occupies the distal two-thirds of the caudal surface of the minor metacarpal (Fig. 9N). It begins on the caudal aspect of the shaft, and extends slightly obliquely to the caudodorsal surface.

The distal ends of the major and minor metacarpals have a fairly restricted contact (approximately 1/6 of the total length), typical of most enantiornithines. This contrasts with the condition observed in forms like *Elsornis* in which the intermetacarpal contact is quite extensive (Chiappe et al., 2007). The major metacarpal is slightly expanded at the distal end, and slightly flattened where it contacts the minor metacarpal (Fig. 9P). The distal condyle of the major metacarpal is non-ginglymoid, with a smooth, rounded articular surface oriented obliquely to that of the carpal trochlea (note: compare orientations of dashed lines 2 and 3 in Fig. 9Q and R, respectively). The minor metacarpal does not expand distally and terminates in a blunt, dorsoventrally compressed condyle (Fig. 9R). This condyle is slightly ginglymoid with a cranio-caudally oriented sulcus (Fig. 9R-1), suggesting a plane of movement different from that at the MP joint of the major metacarpal (Fig. 9R-2).

**Femur**—FMNH PA 752 is a nearly complete, gracile left femur (Fig. 10) recovered from locality MAD 93-18. It is 32.5 mm in length and has a cranio-caudal midshaft diameter of 2.8 mm. The well-defined femoral head is large and nearly spherical (Fig. 10E), and exhibits a large, but shallow depression for the capital ligament on its dorsomedial surface. The head is separated from the trochanteric crest by a long and constricted neck. The femoral head and trochanteric crest assume equivalent proximal positions (Fig. 10A).

There is a small break across the cranio-lateral edge of the proximal femur, resulting in the loss of the cranial portion of the trochanteric crest. Nevertheless, the remaining part of the trochanteric region is present and well preserved. In lateral view, the dorsal margin of the broad trochanteric crest is strongly dorsally arched (Fig. 10D). A well-defined and extensive trochanteric shelf is present on the caudolateral surface below the trochanteric crest (Fig. 10B). Although the cranial margin is incomplete, the trochanteric shelf spans the entire preserved caudal half of the proximal femur. Similar to the dorsal arching of the trochanteric crest, the dorsal margin of the trochanteric shelf is arched. There is a small tubercle on the caudal margin of the trochanteric shelf that is slightly separated from the remainder of the shelf, and may represent the caudal (posterior) trochanter (sensu Hutchinson, 2001) (Fig. 10B). This broad expansion of the trochanteric shelf/caudal trochanter is also seen in enantiornithines (e.g., *Neuquenornis*; Chiappe and Calvo, 1994; Hutchinson, 2001) and *Confusciusornis*. In caudal view, the trochanteric crest is well inset relative to the trochanteric shelf, and a slight groove separates the two features. The lateral surface of femur below the trochanteric shelf is broad and slightly depressed (Fig. 10D).



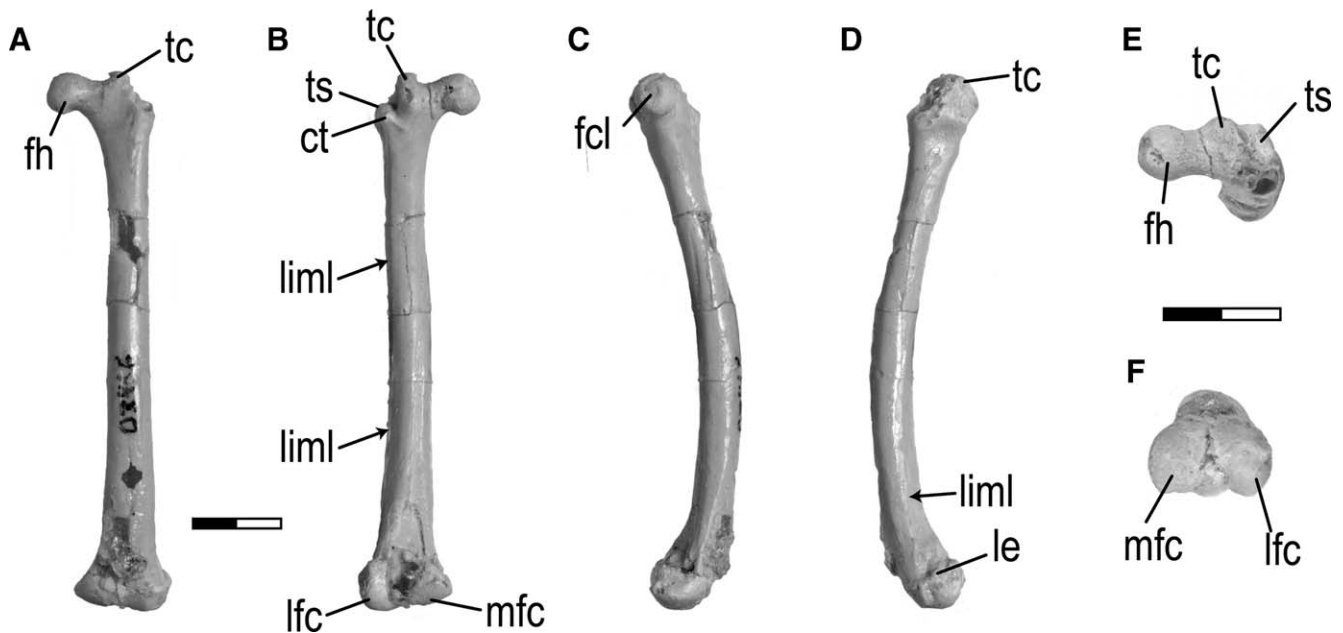


FIGURE 10. Left femur (FMNH PA 752) of *Enantiornithes* indet. in cranial (A), caudal (B), medial (C), lateral (D), proximal (E) and distal (F) views. Caudal and cranial are toward the top of the page in E and F, respectively. **Abbreviations:** ct, caudal (?posterior) trochanter; fcl, capital ligament fossa; fh, femoral head; le, lateral epicondyle; lfc, lateral femoral condyle; liml, lateral intermuscular line; mfc, medial femoral condyle; tc, trochanteric crest; ts, trochanteric shelf. Scale bars equal 0.5 cm.

The femoral shaft is long, gracile, and cranially convex (Fig. 10D); the maximum width of the femur at mid shaft is approximately 8% of its total length. In cranial view the femoral shaft is straight. A distinct muscular scar (the lateral intermuscular line) extends distally from the caudal trochanter down the caudolateral and then lateral margin of the shaft to the lateral epicondyle. This is particularly well defined along the distal half of the shaft (Fig. 10D). There is no cranial intermuscular line and only a poorly defined caudal intermuscular line. The lateral border of the distal shaft projects caudally and is nearly continuous with the lateral condyle (Fig. 10D), characteristic of the situation in many enantiornithines.

The femoral condyles expand modestly to just over twice the midshaft width, and intercondylar and patellar sulci are not evident (Fig. 10A). The medial condyle has a smoothly rounded articular surface (as far as it is preserved) and is flatter than the smaller and more bulbous lateral condyle (Fig. 10B, F). The popliteal fossa is pinched distally (primarily by expansion of the medial condyle), although it is not completely closed off by a transverse ridge of bone (Fig. 10B). The lateral surface of the lateral femoral condyle is impressed with two shallow, irregular depressions. The lateral surface of the distal femur exhibits

a small tubercle topped by a slightly depressed area, the cranial and caudal margins of which are confluent with the lateral intermuscular line (Fig. 10D). A small, rugose area of bone is visible immediately caudal to this depression. This area, along with tubercle itself, likely represent the insertion point of the *ansae m. iliofibularis* as observed in ornithothoracines.

FMNH PA 752 is here referred to enantiornithines based on the following suite of characteristics: the development of a caudally broad, shelf-like caudal trochanter, and the caudal projection of the distolateral border of femoral shaft to the level of the lateral condyle (or ectocondylar tubercle).

**Tibiotarsi**—Two fragmentary tibiotarsi (UA 9752 and UA 6909) have been collected to date, and although of different sized individuals collected from different localities, may both pertain to *Vorona berivotrensis*.

UA 9752 is the proximal one-third of a left tibiotarsus (Fig. 11A–E) recovered from locality MAD 93-36. The preserved portion of UA 9752 is virtually identical to the tibiotarsus of the *Vorona berivotrensis* (Forster et al., 2002), although only approximately 60% the size the holotype (FMNH PA 715). Whereas the proximal articular surface exhibits a craniocaudally elongate medial articular facet, the lateral surface is characterized by a

← FIGURE 9. Antebrachial and carpal elements of *Enantiornithes* indet. and *?Vorona berivotrensis*. Left ulna (UA 9751) (*?Vorona*) in cranial (A), caudal (B), dorsal (C), ventral (D), and proximal (E) views. Partial left ulna (FMNH PA 750) (*?Vorona*) in cranial (F) and ventral (G) views. Proximal right ulna of *Enantiornithes* (UA 9608) in dorsal (H), ventral (I), and proximal (J) views. Proximal right radius (FMNH PA 751) in ventral (K) and proximal (L) views. Left carpometacarpus of *Enantiornithes* indet. (FMNH PA 780) based on  $\mu$ CT scanning and 3D visualization in cranial (M), caudal (N), dorsal (O), ventral (P), proximal (Q), and distal (R) views. Dashed lines in Q and R demarcate the approximate plane of rotation for the proximal and distal joints of the carpometacarpus. Cranial is toward the top of the page in E, Q, and R. **Abbreviations:** alm, alular metacarpal; brf, brachialis fossa; bt, bicipital tubercle; cacf, caudal carpal fovea; cdp, caudodorsal plane; cg, carpal ginglymus; crcf, cranial carpal fovea; dct, dorsal cotyle; dtr, dorsal lip, carpal trochlea; etp, extensor process; icti, intercotylar incisure; ior, interosseous ridge; it, tendinous incisure; ls, longitudinal sulcus; mam, major metacarpal; mim, minor metacarpal; mms, minor metacarpal sulcus; nf, nutrient foramen; olp, olecranon process; pp, pisiform process; rh, radial head; ri, radial incisure; vct, ventral cotyle; vtr, ventral lip, carpal trochlea. 1, 2, and 3 in R indicate approximate plane of rotation at joint surfaces. Scale bar equals 1.0 cm in A–D, 0.5 cm in E, 1.0 cm in F–G, 0.5 cm in H–P, 0.2 cm in Q–R.

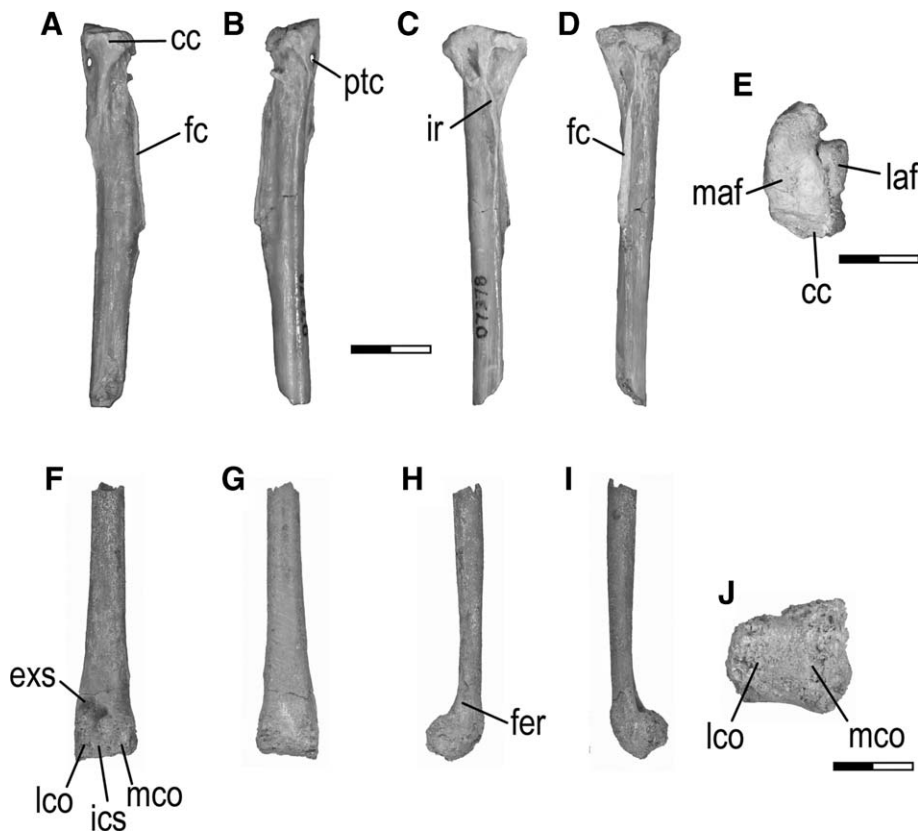


FIGURE 11. Tibiotarsi of *Vorona berivotrensis*. Partial left tibiotarsus (UA 9752) in cranial (A), caudal (B), medial (C), lateral (D), and proximal (E) views. Distal right tibiotarsus (UA 9609) in cranial (F), caudal (G), medial (H), lateral (I), and distal (J) views. Caudal and cranial are toward the top of the page in E and J, respectively. **Abbreviations:** cc, cnemial crest; exs, extensor sulcus; fc, fibular crest; fer, fossa extensor retinaculum; ics, intercondylar sulcus; ir, irregular ridge; laf, lateral articular facet; lco, lateral condyle; maf, medial articular facet; mco, medial condyle; ptc, proximal tibiotarsal canal. Scale bar equals 1.0 cm in A–D and F–I, and 0.5 cm in E and J.

small, sub-triangular facet (Fig. 11E); note, the lateral facet is incomplete along the lateral margin of the facet. A clear separation between the medial and lateral facets is apparent. Similar to FMNH PA 715, UA 9752 exhibits a single, stout, cnemial crest (Fig. 11E) and a low, irregular ridge of bone passing down the medial side of the element from the medial condyle (Fig. 11C). The latter feature is unique to *Vorona* among basal avialans. UA 9752 differs slightly from FMNH PA 715 in that a craniocaudally oriented canal passes through the proximal portion of this ridge (Fig. 11A–B).

UA 9609 is the distal half of a right tibiotarsus (Fig. 11F–J) recovered from locality MAD 93-18. This specimen is also similar to the holotype of *Vorona* (FMNH PA 715), and similar to UA 9752 above, is approximately 60% the size of FMNH PA 715. Notably UA 9609 and UA 9752 are from different localities. The proximal tarsals are completely fused to the tibia, unlike the partial fusion exhibited by FMNH PA 715. The broken shaft of the tibiotarsus is sub-triangular in cross-section, with a flat caudal surface (Fig. 11G). The distal tibia expands only slightly at the transition from the shaft to the condyles. The margins of both condyles are worn and in some areas incomplete. Nevertheless, a number of features are apparent.

In cranial view (Fig. 11F) the medial condyle exceeds the lateral condyle in width by approximately 32%, as in *Vorona* and *Patagopteryx*. The intercondylar sulcus is deep, narrow, and oriented obliquely so that it deviates laterally as it wraps around the distal end. There is a robust medial supracondylar ridge connecting the proximal edge of the medial condyle to the tibial shaft. The lateral supracondylar ridge is narrow and contacts only the lateral-most margin of the lateral condyle, as in *Vorona*, but in contrast to the robust ridge exhibited by *Patagopteryx*. The lateral surface of the lateral supracondylar ridge is developed as a thin, cranio-laterally directed flange (Fig. 11I).

A deep extensor sulcus is present on the cranial surface of the distal tibia between the two supracondylar ridges (Fig. 11F). It is divisible into two distinctive but confluent parts. The first is located just proximal to the lateral condyle, with the second just proximal to the intercondylar incisure. In the floor of the latter is a small circular foramen. There is no osseous supratendinous bridge present. This morphology is identical to that seen in the distal tibia of *Vorona*. In contrast, the distal tibia of *Patagopteryx* bears a single deep extensor sulcus located just proximal to the intercondylar incisure.

The medial surface of the distal tibiotarsus is deeply indented by a medial condylar depression (Fig. 11H). The lateral surface of the lateral condyle bears a moderately deep lateral condylar depression (Fig. 11I). Immediately proximal to the tarsus on the medial and craniomedial surface is an elongate fossa that narrows as it extends proximally up the tibial shaft, ultimately wrapping onto the cranial surface of the element (Fig. 11H). The medial margin of this fossa is formed by a sharp ridge that overhangs it to form a moderately deep, cranially facing groove. The overhanging ridge likely represents the medial attachment site of the extensor retinaculum, rather than forming a distinct tubercle as in other basal avialans (e.g., IGM 100/1311; Clarke and Norell, 2002). Again, this morphology is very similar to that of *Vorona*. However, the medial bounding ridge is less sharply defined distally and does not overhang the fossa to form a groove. The caudal aspect of the distal tibiotarsus is only slightly concave (Fig. 11G) and lacks a well-defined attachment area for the tibial cartilage (i.e., trochlea cartilaginosa tibialis; Baumel and Witmer, 1993).

**Tarsometatarsi**—Tarsometatarsi (TM) are represented by a complete left metatarsus (FMNH PA 782), an unfused, yet associated third and fourth metatarsal (FMNH PA 753), and two isolated first metatarsals (UA 9610, UA 9611).

FMNH PA 782 is a left tarsometatarsus collected from locality MAD 05-42 that preserves fused MT II-IV; the first metatarsal is not preserved. This specimen is 70% the size of the fused tarsometatarsus of the holotype of *Vorona berivotrensis* (UA 8651) but is otherwise generally similar throughout save for a few minor differences. For example, FMNH PA 782 lacks the small dorsal notch between MT II and III (Fig. 12E) present in UA 8651 (Forster et al., 2002:fig. 12.6B). Additionally, FMNH PA 782 exhibits a small, proximally directed hook on the proximodorsal margin of MT II that is absent in UA 8651. UA 8651 does have an expanded shelf at the proximodorsal edge of MT II (Forster et al., 2002:fig.12.6), but this shelf does not exhibit the proximal prong as it does in FMNH PA 782. Although an unfused, splint-like MT V is preserved on the holotype of *Vorona*, this element is absent in FMNH PA 782. FMNH PA 782 does exhibit a small scar along the proximolateral margin, suggesting that a very reduced MT V was present. Forster et al. (2002) hypothesized that the distal tarsals were fused to the metatarsals in UA 8651. Fusion of the proximal end of FMNH PA 782 is so complete that gross observation can neither support nor refute this hypothesis. We refer this specimen to *Vorona berivotrensis*. As with Humeral Taxon A, which may also pertain to *Vorona*, the source of the size variation cannot be determined at present (but see Discussion).

FMNH PA 753 consists of associated but unfused third and fourth left metatarsals collected from locality MAD 93-18. MT IV is extremely reduced relative to MT III. MT IV is approximately 50% the size (in both mediolateral and dorsoplantar dimensions) of MT III (Fig. 12G–J). A distal foramen is present, formed by indentations in the edges of both metatarsals just proximal to the condyles (Fig. 12G–H). The foramen passes directly from dorsal to plantar through the tarsometatarsus as in some avialans (e.g., *Avisaurus*), rather than being partially roofed by one or both metatarsals and/or passing obliquely through the metatarsus (e.g., *Vorona*, see Fig. 12A–B).

The incomplete shaft of MT III is straight and is 25 mm in length. The shaft is slightly broader on the plantar aspect near the distal end of the element (Fig. 12H). The medial surface is flat along the entire contact surface for MT II. The lateral surface is rounded proximally, but flattens distally for contact with MT IV (Fig. 12J). There is a shallow depression on medial surface of the MT IV condyle for contact with MT III; thus, MT III and MT IV contact one another both proximal and distal to the distal foramen (Fig. 12A). Immediately distal to the contact with the medial side of the condyle of MT IV, MT III bears a shallow collateral fossa that is centered on the condyle.

The medial surface of MT III is flat throughout its entire length where it was closely adjacent to MT II. This flattened surface stops at approximately the same point distally as the surface for MT IV (on the lateral side of MT III), at which point MT II and MT III must have diverged. There is no evidence that the condyles of MT II and MT III contacted one another.

The medial surface of the MT III condyle also bears a shallow collateral fossa centered on the condyle (Fig. 12I). The hemicondyles of MT III are very well developed so that in medial view they project dorsal relative to the shaft. In distal view the medial hemicondyle is notably dorsoplantarly expanded relative to the lateral hemicondyle (Fig. 12K). Whereas the two hemicondyles extend the same extent distally, the medial hemicondyle is broader plantarly and extends slightly more proximal than the lateral one. The modestly developed ginglymus is straight and symmetrically bisects the condyles (Fig. 12).

The shaft of MT IV preserves approximately 12.7 mm; however, the proximal end is incomplete. The broken proximal end is dorsoplantarly compressed, with flat dorsal and plantar surfaces. The distal one-third of the shaft deviates laterally, coincident with the location of the distal foramen (Fig. 12A). The medial surface of MT IV is flat until near the level of the distal foramen,

where it assumes a rounded contour. The lateral surface is gently rounded throughout its length. The entire shaft is dorsoplantarly compressed when compared to the depth of MT III; this is the opposite of the condition in *Vorona*.

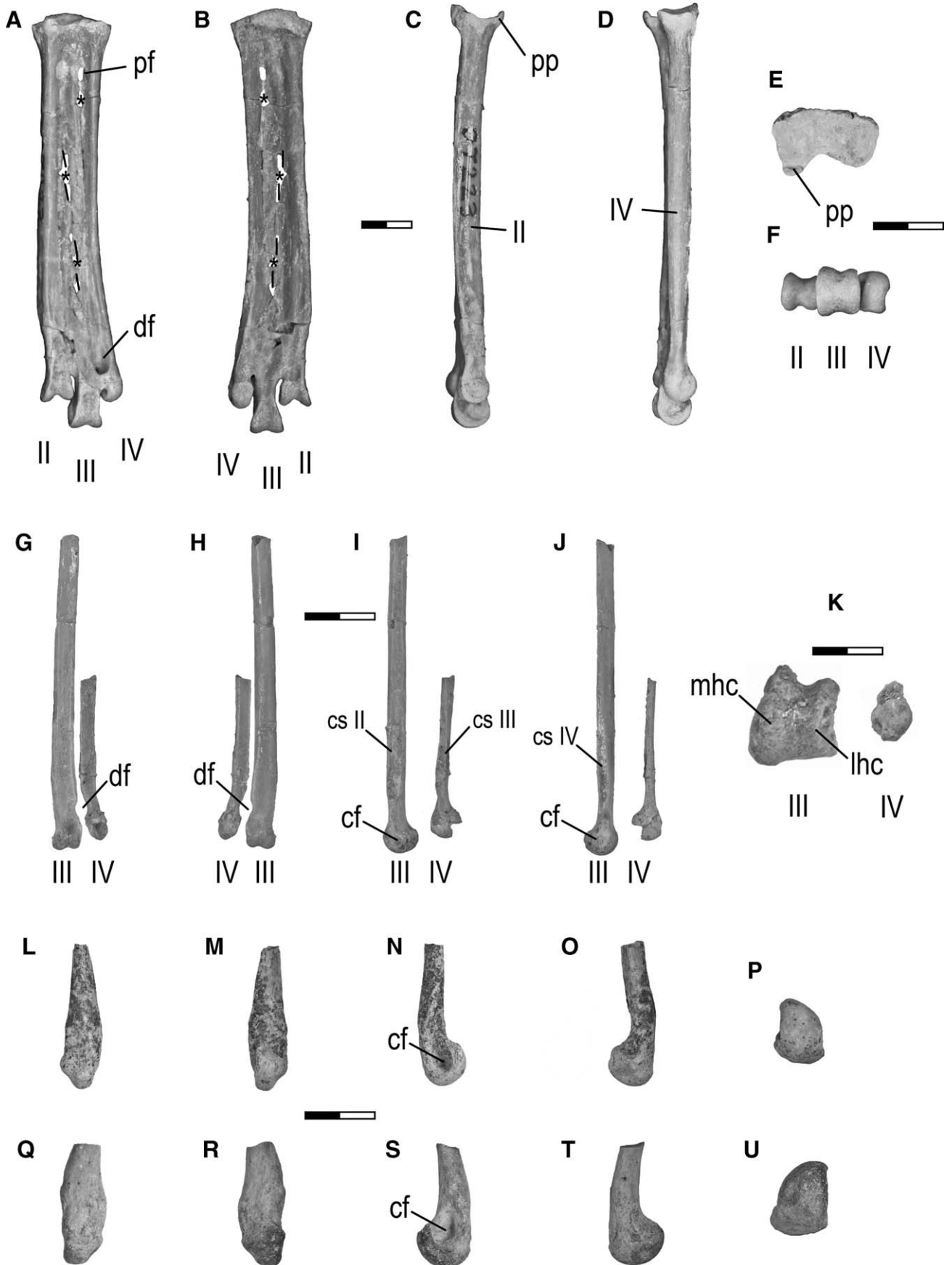
The distal end of MT IV is incomplete, with the dorsodistal aspect of the condyle missing. A small process is present just proximal to the condyle (in-line with the shaft) and is dorsoventrally centered relative to the distal end. A subtle lip is present on the plantomedial margin of the condyle and demarcates a flexor groove (Fig. 12I). The proximal portion of the condyle expands medially to contact MT III distal to the distal foramen. Thus, the medial extension of the MT IV condyle serves to form the intermetatarsal bridge. There are no collateral fossae on either side of the actual condyle and a distinct intercondylar sulcus is not present. The distal end is rounded and globular, with a condyle that is deeper than wide. In medial view the condyle expands equally dorsal and plantar from the shaft, unlike the situation in MT III. FMNH PA 753 is tentatively referred to enantiornithes based on exhibiting an MT IV that is narrower (mediolaterally) than MT III (Chiappe, 1993; Zhou et al., 2008). FMNH PA 753 is notable even among enantiornithines in its degree of craniocaudal restriction (Fig. 12J). Taken together, the features present (e.g., relative dimensions of the MT III and MT IV shafts, trochlear morphology of MT III) in FMNH PA 753 are generally similar to the enantiornithines *Avisaurus* and *Soroavisaurus* (Chiappe, 1992, 1993; Chiappe and Calvo, 1994; Chiappe and Walker, 2002). More complete materials are necessary to further refine this assignment.

UA 9610 is a left first metatarsal (Fig. 12L–P) collected from locality MAD 93-18. It is missing the proximal end of its shaft. The remaining metatarsal shaft is compressed and tapered proximally. The shaft is slightly twisted such that it suggests the presence of a partial reversion of the hallux. The shaft is dorsoplantarly compressed (Fig. 12N). The plantar surface of the shaft and condyle are slightly convex; thus the entire element lacks the strong 'J-shaped' morphology characteristic of enantiornithines (e.g., *Soroavisaurus*, *Neuquenornis*). The condyle is slightly narrower than the width of the distal shaft (Fig. 12M), but expands dorsally to approximately twice the dorsoplantar dimensions of the distal shaft (Fig. 12N). In distal view the condyle is narrow dorsally, expanded mediolaterally along the ventral margin, and unequally divided by a ginglymus (Fig. 12P). The condylar articular surface is otherwise globose and oriented approximately 45 degrees offset from the long axis of the shaft (Fig. 12M). A large and deep collateral fossa occupies the entire medial side of the condyle (Fig. 12N).

UA 9611 is a right first metatarsal (Fig. 12Q–U) recovered from locality MAD 93-18 and is slightly larger than UA 9610. Similar to UA 9610, UA 9611 is also missing the proximal portion of the shaft; however, given the distal position of the break, it cannot be determined whether the shaft was twisted. Other than size, the morphology of this specimen is nearly identical to that of UA 9610.

## DISCUSSION

Field research conducted since 1993 has yielded a growing diversity of avialan theropods from the Maevarano Formation (Forster et al., 1996, 1998; Forster and O'Connor, 2000). The large number of isolated specimens (32) recovered from the formation suggest that avialans were relatively common within this Maastrichtian vertebrate assemblage. The 13 partial to complete humeri alone indicate that a minimum of six different species were present. Two of these (Humeral Taxon A and Humeral Taxon B) belong to fairly large forms, whereas the others pertain to much smaller birds, the largest taxon being nearly seven times the size of the smallest (humeral midshaft diameters range from 1.3 to 9.5 mm). Moreover, the large synsacrum (FMNH



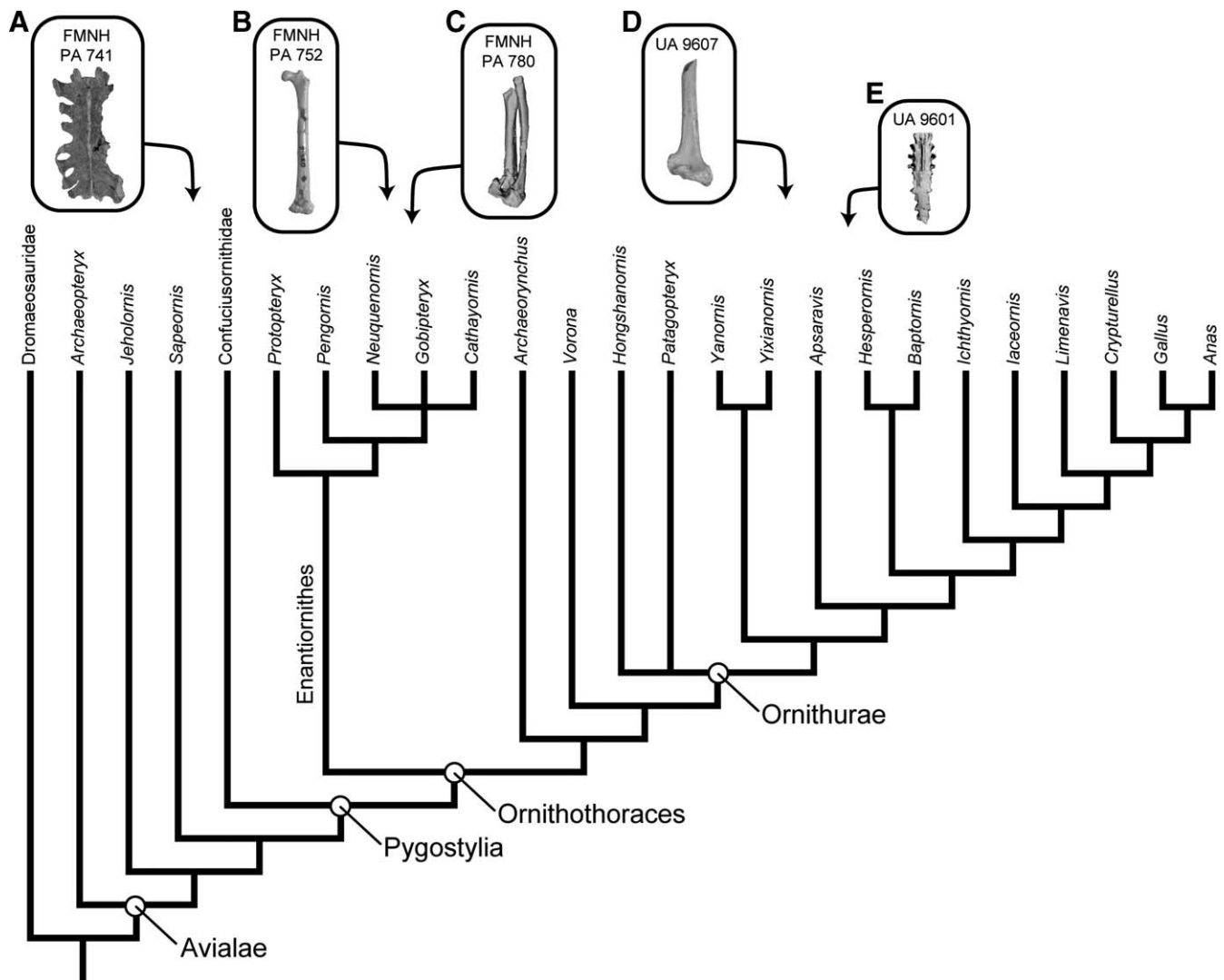


FIGURE 13. Summary diagram to highlight the diversity of Maevarano Formation avialans, including a nonpygostylian/basal pygostylian synsacrum (A), an enantiornithine femur (B), an enantiornithine carpometacarpus (C), an ornithurine distal humerus (D), and an ornithurine synsacrum (E). Phylogenetic nomenclature based on Gauthier and de Queiroz (2001) and Chiappe and Witmer (2002), and reference topology modified from recent analyses of Zhou et al. (2008) and O'Connor et al. (2009). Note: elements are not to scale—see main figures for detailed size and morphological information.

PA 741; Figs. 2, 13), based on its estimated phylogenetic position and similarities with *Sapeornis* (see discussion below), is unlikely to pertain to Humeral Taxon A, *Vorona*, because the latter clearly represents an ornithothoracine (see below). Moreover, its dissimilarity to the known synsacrum of Humeral Taxon B, *Rahonavis*, precludes its referral to this taxon. It therefore

represents a seventh Maevarano avialan. Within the Maevarano vertebrate fauna, this relatively high diversity in avialans is equaled only by that of crocodyliforms, where seven taxa are currently recognized (Krause et al., 1997, 2006). Both avialans and crocodyliforms are each more diverse than any other vertebrate clade in the Maevarano Formation, including nonavian

← FIGURE 12. Metatarsals of Avialae. Left tarsometatarsus (FMNH PA 782) of *Vorona berivotrensis* in dorsal (A), plantar (B), medial (C), lateral (D), proximal (E), and distal (F) views. Associated left MT III and MT IV (FMNH PA 753) of *Enantiornithes* indet. in dorsal (G), plantar (H), medial (I), lateral (J), and distal (K) views. Left first (MT I) metatarsal (UA 9610) of Avialae indet. in dorsal (L), plantar (M), medial (N), lateral (O), and distal (P) views. Right first (MT I) metatarsal (UA 9611) in dorsal (Q), plantar (R), medial (S), lateral (T), and distal (U) views. Caudal is towards the top of the page in E, cranial is toward the top of the page in F, K, P, and U. **Abbreviations:** II, 2nd metatarsal; III, 3rd metatarsal; IV, 4th metatarsal; cf, collateral fossa; cs II, contact surface for 2nd metatarsal; cs III, contact surface for 3rd metatarsal; cs IV, contact surface for 4th metatarsal; df, distal foramen; lhc, lateral hemicondyle; mhc, medial hemicondyle; pf, proximal foramen; pp, proximal process; black asterisks in A and B indicated areas of broken bone. Scale bar equals 0.5 cm in A–F, 1.0 cm in G–J, 0.2 cm in K, and 1.0 cm in L–U.

dinosaurs, where only four taxa are known (two abelisauroid theropods, two titanosaurian sauropods).

Because nearly all of the avialans described herein were recovered as isolated elements, identifications of and associations among most specimens are difficult to affirm. For example, the small synsacrum (UA 9601) possesses morphology (10 fused sacral vertebrae, midseries sacral vertebrae subequal in length) suggesting affinities with ornithurine birds generally, and perhaps even a close association with forms like *Apsaravis* (Fig. 13). The two small distal humeri (UA 9607, FMNH PA 748; 'Humeral Taxa Unknown') also exhibit features (e.g., incipient scapulotricipital sulcus, well-defined dorsal supracondylar tubercle) suggesting broadly similar phylogenetic affinities. However, in lieu of articulated or directly associated remains, it is impossible to ascertain whether the synsacrum is from the same species as either of the humeri.

Despite problems of identification and association due to the recovery of isolated materials, some morphological evidence suggests that two of the humeral taxa (A and B) pertain to previously named and described Maevarano avialans. The morphology of Humeral Taxon B (FMNH PA 746, UA 9604; Fig. 5) indicates that it (1) pertains to a very primitive avialan, (2) is size-consistent with *Rahonavis ostromi*, and (3) demonstrates perfectly congruent articulations with the known proximal ulna of *Rahonavis* (Forster et al., 1998). Thus, a number of lines of evidence provide the basis for referring these two specimens to *R. ostromi*. However, we caution that this assignment is not through direct association, but rather, is based solely on morphological criteria. In contrast, the morphology of Humeral Taxon A is consistent with a phylogenetic assignment among derived nonornithurine, ornithothoracine birds (possibly within enantiornithines), and is size-consistent with *Vorona berivotrensis*. Humeral Taxon A and the described hind limb material of *Vorona* represent, by far, the largest Maevarano avialan materials, exceeding *Rahonavis* in size by approximately 42%. Thus, we tentatively refer Humeral Taxon A to *Vorona*, again with the caveat that this referral remains an untested hypothesis until articulated/associated materials are recovered.

Based only on the taxa discussed above (Humeral Taxon A, Humeral Taxon B, and 'Unknown'; two distinct synsacra), it is evident that the Maevarano avifauna represents a phylogenetically diverse assemblage, including very primitive avialans (*Rahonavis*; the large synsacrum, FMNH PA 741), a derived, large-bodied nonornithurine (*Vorona*), and at least one ornithurine (the small synsacrum, UA 9601; Humeral Taxon Unknown, UA 9607) (see Fig. 13). Moreover, by examining other Maevarano avialans, it is possible to posit a preliminary phylogenetic position (Fig. 13) based on character distributions from existing phylogenetic analyses (e.g., Zhou et al., 2008). For example, the large synsacrum (FMNH PA 741) shares a number of characters with *Sapeornis* and appears to belong to a non-ornithothoracine avialan. A number of other isolated elements (e.g., carpometacarpus, FMNH PA 780; Humeral Taxon C, FMNH PA 747; Humeral Taxon D, UA 9605; femur, FMNH PA 752; tarsometatarsus, FMNH PA 753) possess characters suggesting that they pertain to enantiornithine birds, or at least to basal ornithothoracines. In summary, the seven Maevarano Formation avialans (minimally) span a phylogenetic range from extremely primitive non-ornithothoracines to more derived ornithurines, with representatives from most intervening clades (Fig. 13).

Such a diversity of 'archaic' birds in this single, latest Cretaceous avifauna is significant in two respects. First, it demonstrates that multiple clades of basal (non-neornithine) birds persisted until at least near the end of the Mesozoic, suggesting that the end-Cretaceous mass extinction event had a significant impact on basal avialans, perhaps more so than previously recognized (Feduccia, 1999; Chiappe and Witmer, 2002). In other words, a number of basal avialan clades known since the Early Cretaceous

not only co-existed (at least on Madagascar), but did so until the latest stage of the Mesozoic Era. Second, the absence of Neornithes (modern birds) is interesting in that a number of molecular studies (e.g., Cooper and Penny, 1997; van Tuinen and Hedges, 2001) have predicted the existence of a vast neornithine diversification during the Cretaceous. Moreover, specific hypotheses based on phylogenetic and historical biogeographic inferences suggesting a Gondwana-centered neornithine radiation during the Cretaceous (Cracraft, 2001) are also not supported by the Maevarano avifauna. It may be the case that the Maevarano birds represent a relictual assemblage of basal clades that survived on Madagascar as it became increasingly isolated from other Gondwanan landmasses during the Cretaceous (see Storey et al., 1995; Reeves and de Wit, 2000; Rotstein et al., 2001). However, given the Gondwanan-wide cosmopolitanism evidenced by a number of other terrestrial clades (e.g., frogs, nonavian dinosaurs, mammals) that are also present in the Maevarano assemblage (Krause et al., 2006; Evans et al., 2008), it is even more interesting to note the absence of a volant clade (Neornithes) that would have been even less restricted than large-bodied (e.g., dinosaurs) or marine-intolerant (e.g., frogs) terrestrial forms to using subaerial connections as dispersal routes. Finally, from a general biogeographic perspective, the Maevarano bird assemblage, one that is dominated by enantiornithines and other non-ornithurine forms, most closely resembles avifaunas known from the Late Cretaceous of Argentina (Chiappe and Walker, 2002), and thus, illustrates at least basic congruence with many of the biogeographic patterns apparent among other Late Cretaceous terrestrial taxa (Krause et al., 2006). This is in sharp contrast to the mixed enantiornithine-ornithurine and ornithurine-dominated assemblages known from Cretaceous units in North American and Asia (Hope, 2002; Clarke and Norell, 2004; Clarke et al., 2006; Zhou and Zhang, 2006).

The phylogenetic diversity of Maevarano avialans is matched by a large range of body sizes, with humeral midshaft diameters (dorsoventral) spanning from 1.3 to 9.5 mm, corresponding to estimated total humeral lengths ranging between 19 and 120 mm and therefore equivalent to the range in sizes represented among extant taxa by *Spizella arborea* (American tree sparrow) and *Buteo jamaicensis* (red-tailed hawk). This is an estimated seven-fold difference in sizes among avialans within a single Maastrichtian avifauna.

One of the more interesting aspects of size variability concerns *Vorona berivotrensis*. Previously described materials of this taxon include identically sized left and right femora, tibiotarsi, and a single metatarsus (Forster et al., 1996, 2002). Additional material tentatively assigned to *Vorona* (see above) is described herein and includes two partial tibiotarsi (UA 9752, UA 6909), a left tarsometatarsus (FMNH PA 782), five partial humeri (FMNH PA 743, FMNH PA 744, FMNH PA 745, UA 9705, UA 9749) and two ulnae (FMNH PA 750, UA 9751). For these elements (humeri, ulnae, tibiotarsi, tarsometatarsi), each is represented by two different size classes: a larger (similar in size to the holotype) and smaller morph. Importantly, these size differences are consistent within elements where two or more specimens of the smaller morph are present. For example, the two partial tibiotarsi of the smaller morph are both 60% the size of the larger morph, and the three partial humeri of the smaller morph are all approximately 80% the size of the larger morph. For the two elements where multiple smaller morph specimens are not present, the smaller metatarsal morph is 70% the size of the larger morph, and the smaller ulna morph is 65% the size of the larger morph. The recognition of multiple examples of similar-sized smaller morphs suggests that size-class differences are likely not due to ontogenetic staging, but may instead relate to either sexual dimorphism within a single taxon or interspecific variability between closely related species. If the latter, the taxonomic diversity of the Maevarano avifauna is even more diverse than estimated above.

The larger and smaller humeral morphs are identical to one another, at least in their overlapping preserved morphology (Fig. 4). The two ulnar morphs are also identical, although neither is well preserved (Fig. 9A–G). Among tibiotarsi, there are some slight differences between the partial smaller morph specimens and the previously described larger morph specimens. For example, smaller morph UA 9752 has a small canal traversing the 'irregular ridge' that characterizes the taxon (Fig. 11), a feature absent in the larger morph. Smaller morph UA 9609 also exhibits complete fusion of the tarsals to the distal tibia (Fig. 11F), unlike the partial fusion of the larger morph (e.g., FMNH PA 715; Forster et al., 2002). Fusion of smaller morph UA 9609 also suggests that it represents a skeletally mature individual.

Subtle differences are also manifest between the smaller and larger morphs of the tarsometatarsi. For example, the smaller morph (FMNH PA 782; Fig. 12A–E) lacks the small dorsal notch between MT II and III that is present in the larger morph (UA 8651). Also, the smaller morph exhibits a proximally projecting hook on the proximodorsal margin of MT II (Fig. 12E), a trait that is less obvious in UA 8651. As with the size class differences, it is not currently possible to ascertain whether such subtle morphological variation represents sexual dimorphism, taxonomic differences between closely related species, or simply individual variation within a species for which a suitable sample size is still lacking.

Interestingly, the size differences between the larger and smaller morphs vary among the four limb elements, ranging from 60% (tibiotarsi) to 70% (tarsometatarsi) to 72% (ulnae) to 80% (humeri). If two adult size classes are recognized in *Vorona*, they may include not just size differences, but proportional differences among parts of the skeleton as well. However, unlike the situation with the humeri and tibiotarsi, there is no 'internal check' on the consistency of the size differences for the tibiotarsi and ulnae, as only one larger and one smaller morph are known for both these elements. Nevertheless, the humeri and tibiotarsi form the endpoints for the range of size differences in *Vorona*. Assuming the size differences reported above characterize the two morphs, then the smaller morph would not only be smaller in size, but would have relatively shorter hind limb and antibrachial elements than the larger morph. Both interlimb and intralimb scaling patterns are significant in the context of growth dynamics (e.g., related to identification of intraspecific dimorphism), locomotor potential (e.g., the origin/evolution of the modern avian flight apparatus), and our growing appreciation regarding the ecological diversification among Mesozoic avialans (e.g., Clarke et al., 2006; Chiappe et al., 2007; Zhou et al., 2008). The ever-growing sample of Maevarano Formation avialans will no doubt contribute to these and other questions if more complete, associated skeletons can be recovered.

#### ACKNOWLEDGMENTS

We thank D. W. Krause for his continued support and skilled leadership over the course of the Mahajanga Basin Project. The extensive excavations at localities MAD 93-18 and MAD 05-42 were conducted over many field seasons. We thank all expedition members who participated in the MAD 93-18 excavations in 1995, 1996, 1998, 1999, 2003, and 2005, and the MAD 05-42 excavations in 2005 and 2007. We also thank the following individuals: J. Groenke and V. Heisey for specimen preparation; M. Stewart, J. Sattler, J. Sidote, and M. Graham for photography and digital image assistance; L. Betti-Nash for assistance with Figure 1; L. Chiappe for access to his extensive collection of Mesozoic birds and numerous discussions; J. Clarke, G. Dyke, and J. Harris for discussions, information, and data matrices on Mesozoic birds. Three anonymous reviewers are thanked for the constructive comments on the original submission of this contribu-

tion. This work was supported by the National Science Foundation (DEB-9224396, EAR-9418816, EAR-9706302, EAR-106477, EAR-116517, EAR-0446488, and EAR-0617561), the National Geographic Society, the Dinosaur Society, the Ohio University Office of Research and Sponsored Programs, and the Ohio University College of Osteopathic Medicine.

#### LITERATURE CITED

- Baumel, J. J. 1993. Handbook of Avian Anatomy: Nomina Anatomica Avium. Nuttall Ornithological Club, Cambridge, U.K., 779 pp.
- Baumel, J. J., and L. M. Witmer. 1993. Osteologia; pp. 45–132 in J. J. Baumel (ed.), Handbook of Avian Anatomy: Nomina Anatomica Avium. Nuttall Ornithological Club, Cambridge, U.K.
- Buffetaut, E., J. Le Loeuff, P. Mechin, and A. Mechin-Salessy. 1995. A large French Cretaceous bird. *Nature* 377:110.
- Chiappe, L. M. 1992. Enantiornithine (aves) tarsometatarsi and the avian affinities of the Late Cretaceous Avisauridae. *Journal of Vertebrate Paleontology* 12:344–350.
- Chiappe, L. M. 1993. Enantiornithine (Aves) tarsometatarsi from the Cretaceous Lecho Formation of Northwestern Argentina. *American Museum Novitates* 3083:1–27.
- Chiappe, L. M. 1995. The first 85 million years of avian evolution. *Nature* 378:349–355.
- Chiappe, L. M. 1996a. Early avian evolution in the southern hemisphere: the fossil record of birds in the Mesozoic of Gondwana. *Memoirs of the Queensland Museum* 39:533–554.
- Chiappe, L. M. 1996b. Late Cretaceous birds of southern South America: anatomy and systematics of Enantiornithes and *Patagopteryx deferrariisi*; pp. 203–244 in G. Arratia (ed.), Contributions of Southern South America to Vertebrate Paleontology. *Münchner Geowissenschaftliche Abhandlungen (A)* 30. Verlag, Dr. Pfeil, Munich, Germany.
- Chiappe, L. M. 2002. Basal bird phylogeny: problems and solutions; pp. 448–472 in L. M. Chiappe and L. M. Witmer (eds.), *Mesozoic Birds: Above the Heads of Dinosaurs*. University of California Press, Berkeley, California.
- Chiappe, L. M., and J. O. Calvo. 1994. *Neuquenornis volans*, a new Late Cretaceous bird (Enantiornithes: Avisauridae) from Patagonia, Argentina. *Journal of Vertebrate Paleontology* 14:230–246.
- Chiappe, L. M., and G. J. Dyke. 2002. The Mesozoic radiation of birds. *Annual Review of Ecology and Systematics* 33:91–124.
- Chiappe, L. M., and C. A. Walker. 2002. Skeletal morphology and systematics of the Cretaceous Euenantiornithes (Ornithothoraces: Enantiornithes); pp. 240–267 in L. M. Chiappe and L. M. Witmer (eds.), *Mesozoic Birds: Above the Heads of Dinosaurs*. University of California Press, Berkeley, California.
- Chiappe, L. M., and L. M. Witmer. 2002. *Mesozoic Birds: Above the Heads of Dinosaurs*. University of California Press, Berkeley, California, 520 pp.
- Chiappe, L. M., J. P. Lamb Jr., and P. G. P. Ericson. 2002. New enantiornithine bird from the marine Upper Cretaceous of Alabama. *Journal of Vertebrate Paleontology* 22:170–174.
- Chiappe, L. M., M. A. Norell, and J. M. Clark. 2001. A new skull of *Gobipteryx minuta* (Aves: Enantiornithes) from the Cretaceous of the Gobi desert. *American Museum Novitates* 3346:1–15.
- Chiappe, L. M., S.-A. Ji, Q. Ji, and M. A. Norell. 1999. Anatomy and systematics of the Confuciusornithidae (Theropoda: Aves) from the Late Mesozoic of northeastern China. *Bulletin of the American Museum of Natural History* 242:1–89.
- Chiappe, L. M., S. Suzuki, G. J. Dyke, M. Watabe, K. Tsogbaatar, and R. Barsbold. 2007. A new enantiornithine bird from the Late Cretaceous of the Gobi Desert. *Journal of Systematic Paleontology* 5:193–208.
- Clark, J. A., M. A. Norell, and P. J. Makovicky. 2002. Cladistic approaches to the relationships of birds to other theropod dinosaurs; pp. 46–67 in L. M. Chiappe and L. M. Witmer (eds.), *Mesozoic Birds: Above the Heads of Dinosaurs*. University of California Press, Berkeley, California.
- Clarke, J. A., and L. M. Chiappe. 2001. A new carinate bird from the Late Cretaceous of Patagonia (Argentina). *American Museum Novitates* 3323:1–23.
- Clarke, J. A., and M. A. Norell. 2002. The morphology and phylogenetic position of *Apsaravis ukhaana* from the Late Cretaceous of Mongolia. *American Museum Novitates* 3387:1–46.

- Clarke, J. A., and M. A. Norell. 2004. New avialan remains and a review of the known avifauna from the Late Cretaceous Nemegt Formation of Mongolia. *American Museum Novitates* 3447:1–12.
- Clarke, J. A., Z.-H. Zhou, and F.-C. Zhang. 2006. Insight into the evolution of avian flight from a new clade of Early Cretaceous ornithurines from China and the morphology of *Yixianornis grabaui*. *Journal of Anatomy* 208:287–308.
- Clarke, J. A., C. P. Tambussi, J. I. Noriega, G. M. Erickson, and R. A. Ketchum. 2005. Definitive fossil evidence for the extant avian radiation in the Cretaceous. *Nature* 433:305–308.
- Cooper, A., and D. Penny. 1997. Mass survival of birds across the Cretaceous-Tertiary boundary: molecular evidence. *Science* 275:1109–1113.
- Cracraft, J. 2001. Avian evolution, Gondwana biogeography and the Cretaceous-Tertiary mass extinction event. *Proceedings of the Royal Society of London B* 268:459–469.
- Dalla Vecchia, F. M., and L. M. Chiappe. 2002. First skeleton from the Mesozoic of Northern Gondwana. *Journal of Vertebrate Paleontology* 22:856–860.
- Dyke, G. J., and M. van Tuinen. 2004. The evolutionary radiation of modern birds (Neornithes): reconciling molecules, morphology, and the fossil record. *Zoological Journal of the Linnean Society* 141:153–177.
- Evans, S. E., M. E. H. Jones, and D. W. Krause. 2008. A giant frog with South American affinities from the Late Cretaceous of Madagascar. *Proceedings of the National Academy of Sciences of the United States of America* 105:2951–2956.
- Feduccia, A. 1999. *The Origin and Evolution of Birds*. Yale University Press, New Haven, 466 pp.
- Forster, C. A., and P. M. O'Connor. 2000. The avifauna of the Upper Cretaceous Maevarano Formation, Madagascar. *Journal of Vertebrate Paleontology* 20:41A–42A.
- Forster, C. A., L. M. Chiappe, D. W. Krause, and S. D. Sampson. 1996. The first Cretaceous bird from Madagascar. *Nature* 382:532–534.
- Forster, C. A., L. M. Chiappe, D. W. Krause, and S. D. Sampson. 2002. *Vorona berivotrensis*, a primitive bird from the Late Cretaceous of Madagascar; pp. 268–280 in L. M. Chiappe and L. M. Witmer (eds.), *Vorona berivotrensis*. University of California Press, Berkeley, California.
- Forster, C. A., S. D. Sampson, L. M. Chiappe, and D. W. Krause. 1998. The theropod ancestry of birds: new evidence from the Late Cretaceous of Madagascar. *Science* 279:1915–1919.
- Gauthier, J., and K. de Queiroz. 2001. Feathered dinosaurs, flying dinosaurs, crown dinosaurs, and the name “Aves”; pp. 7–41 in J. Gauthier and L. F. Gall (eds.), *New Perspectives on the Origin and Early Evolution of Birds*. Peabody Museum of Natural History, New Haven.
- Gauthier, J., and L. F. Gall. *New Perspectives on the Origin and Early Evolution of Birds*. Peabody Museum of Natural History, New Haven, 613 pp.
- Hope, S. 2002. The Mesozoic radiation of Neornithes; pp. 339–388 in L. M. Chiappe and L. M. Witmer (eds.), *Mesozoic Birds: Above the Heads of Dinosaurs*. University of California Press, Berkeley, California.
- Hou, L., L. D. Martin, Z. Zhou, and A. Feduccia. 1996. Early adaptive radiation of birds: evidence from fossils from Northeastern China. *Science* 274:1164–1167.
- Hou, L., L. M. Chiappe, F. Zhang, and C. Chuong. 2004. New Early Cretaceous fossil from China documents a novel trophic specialization for Mesozoic birds. *Naturwissenschaften* 91:22–25.
- Hutchinson, J. R. 2001. The evolution of femoral osteology and soft tissues on the line to extant birds (Neornithes). *Zoological Journal of the Linnean Society* 131:169–197.
- Ji, Q., L. M. Chiappe, and S.-A. Ji. 1999. A new late Mesozoic confuciusornithid bird from China. *Journal of Vertebrate Paleontology* 19:1–7.
- Krause, D. W., J. H. Hartman, and N. A. Wells. 1997. Late Cretaceous vertebrates from Madagascar: implications for biotic change in deep time; pp. 2–43 in S. D. Goodman and B. D. Patterson (eds.), *Natural Change and Human Impact in Madagascar*. Smithsonian Institution Press, Washington D.C.
- Krause, D. W., P. M. O'Connor, K. C. Rogers, S. D. Sampson, G. A. Buckley, and R. R. Rogers. 2006. Late Cretaceous terrestrial vertebrates from Madagascar: implications for Latin American Biogeography. *Annals of the Missouri Botanical Garden* 93:178–208.
- Kurochkin, E. N., G. J. Dyke, and A. A. Karhu. 2002. A new presbyornithid bird (Aves, Anseriformes) from the late cretaceous of southern Mongolia. *American Museum Novitates* 3386:1–11.
- Lamanna, M. C., H. You, J. D. Harris, L. M. Chiappe, S. Ji, J. Lu, and Q. Ji. 2006. A partial skeleton of an enantiornithine bird from the Early Cretaceous of northwestern China. *Acta Palaeontologica Polonica* 51:423–434.
- Livezey, B. C., and R. L. Zusi. 2006. Higher-order phylogeny of modern birds (Theropoda, Aves: Neornithes) based on comparative anatomy: I. Methods and characters. *Bulletin of Carnegie Museum of Natural History* 37:1–544.
- Mayr, G., and J. Clarke. 2003. The deep divergences of neornithine birds: a phylogenetic analysis of morphological characters. *Cladistics* 19:527–553.
- Makovicky, P., S. Apesteguia, and F. L. Agnolin. 2005. The earliest dromaeosaurid theropod from South America. *Nature* 437:1007–1011.
- Molnar, R. E. 1986. An enantiornithine bird from the Lower Cretaceous of Queensland, Australia. *Nature* 322:736–738.
- Necker, R. 1999. Specializations in the lumbosacral spinal cord of birds: morphological and behavioural evidence for a sense of equilibrium. *European Journal of Morphology* 37:211–214.
- Necker, R. 2005. The structure and development of avian lumbosacral specializations of the vertebral canal and the spinal cord with special reference to a possible function as a sense organ of equilibrium. *Anatomy and Embryology* 210:59–74.
- Necker, R. 2006. Specializations in the lumbosacral vertebral canal and spinal cord of birds: evidence of a function as a sense organ which is involved in the control of walking. *Journal of Comparative Physiology A* 192:439–448.
- Nesbitt, S. J., A. H. Turner, M. Spaulding, J. L. Conrad, and M. A. Norell. 2009. The theropod furcula. *Journal of Morphology* 270:856–879.
- Nessov, L. A. 1992. Mesozoic and Paleogene birds of the USSR and their paleoenvironments; pp. 465–478 in K. E. Campbell, Jr. (ed.), *Papers in Avian Paleontology Honoring Pierce Brodkorb*, Los Angeles County Museum of Natural History, Science Series.
- Norell, M. A., and J. A. Clarke. 2001. Fossil that fills a critical gap in avian evolution. *Nature* 409:181–184.
- Norell, M. A., J. M. Clark, A. H. Turner, P. Makovicky, R. Barsbold, and T. Rowe. 2006. A new dromaeosaurid theropod from Ukhua Tolgod (Omnogov, Mongolia). *American Museum Novitates* 3545:1–51.
- Noriega, J. I., and C. P. Tambussi. 1995. A Late Cretaceous Presbyornithidae (Aves: Anseriformes) from Vega Island, Antarctic Peninsula: paleobiogeographic implications. *Ameghiniana* 32:57–61.
- Novas, F. E., D. Pol, J. I. Canale, J. D. Porfiri, and J. O. Calvo. 2008. A bizarre Cretaceous theropod dinosaur from Patagonia and the evolution of Gondwanan dromaeosaurids. *Proceedings of the Royal Society B* 276:1101–1107.
- O'Connor, J. K., X. Wang, L. M. Chiappe, C. Gao, Q. Meng, X. Cheng, and J. Liu. 2009. Phylogenetic support for a specialized clade of Cretaceous enantiornithine birds with information from a new species. *Journal of Vertebrate Paleontology* 29:188–204.
- Reeves, C., and M. de Wit. 2000. Making ends meet in Gondwana: retracing the transforms of the Indian Ocean. *Terra Nova* 12:272–280.
- Rogers, R. R. 2005. Fine-grained debris flows and extraordinary vertebrate burials in the Late Cretaceous of Madagascar. *Geology* 33:297–300.
- Rogers, R. R., J. H. Hartman, and D. W. Krause. 2000. Stratigraphic analysis of Upper Cretaceous rocks in the Mahajanga Basin, Northwestern Madagascar: implications for ancient and modern faunas. *Journal of Geology* 108:275–301.
- Rotstein, Y., M. Munschy, and A. Bernard. 2001. The Kerguelen Province revisited: additional constraints on the early development of the Southeast Indian Ocean. *Marine Geophysical Researches* 22:81–100.
- Sanz, J. L. 1992. A new bird from the Early Cretaceous of Las Hoyas, Spain, and the early radiation of birds. *Palaeontology* 35:829–845.
- Sanz, J. L., L. M. Chiappe, and A. D. Buscalioni. 1995. The osteology of *Concornis lacustris* (Aves: Enantiornithes) from the Lower Cretaceous of Spain and a reexamination of its phylogenetic relationships. *American Museum Novitates* 3133:1–23.
- Sanz, J. L., L. M. Chiappe, B. P. Pérez-Moreno, A. D. Buscalioni, J. J. Moratalla, F. Ortega, and F. J. Poyato-Ariza. 1996. An Early

- Cretaceous bird from Spain and its implications for the evolution of avian flight. *Nature* 382:442–445.
- Sanz, J. L., L. M. Chiappe, B. P. Pérez-Moreno, J. J. Moratalla, F. Hernández-Carrasquilla, A. D. Buscalioni, F. Ortega, F. J. Poyato-Ariza, D. Rasskin-Gutman, and X. Martínez-Delclòs. 1997. A nestling bird form the Lower Cretaceous of Spain: implications for avian skull and neck evolution. *Science* 276:1543–1546.
- Sereno, P. C. 2000. *Iberomesornis romerali* (Aves, Ornithothoraces) reevaluated as an Early Cretaceous enantiornithine. *Neues Jahrbuch für Geologie und Paläontologie Abhandlungen* 215:365–395.
- Sereno, P. C., and C. Rao. 1992. Early evolution of avian flight and perching: new evidence from the Lower Cretaceous of China. *Science* 255:845–848.
- van Tuinen, M., and S. B. Hedges. 2001. Calibration of avian molecular clocks. *Molecular Biology and Evolution* 18:206–218.
- Varricchio, D. J., and L. M. Chiappe. 1995. A new enantiornithine bird from the Upper Cretaceous two medicine formation of Montana. *Journal of Vertebrate Paleontology* 15:201–204.
- Walker, C. A., E. Buffetaut, and G. J. Dyke. 2007. Large euenantiornithine birds from the Cretaceous of southern France, North America and Argentina. *Geological Magazine* 144:977–986.
- You, H., M. C. Lamanna, J. D. Harris, L. M. Chiappe, J. K. O'Connor, S. Ji, J. Lu, C. Yuan, D. Li, X. Zhang, K. J. Lacovara, P. Dodson, and Q. Ji. 2006. A nearly modern amphibious bird from the Early Cretaceous of northwestern China. *Science* 312:312–315.
- Zhang, F.-C., and Z.-H. Zhou. 2000. A primitive enantiornithine bird and the origin of feathers. *Science* 290:1955–1959.
- Zhou, Z.-H., and F.-C. Zhang. 2002. A long-tailed, seed-eating bird from the Early Cretaceous of China. *Nature*:405–409.
- Zhou, Z.-H., and F.-C. Zhang. 2003. Anatomy of the primitive bird *Sapeornis chaoyangensis* from the Early Cretaceous of Liaoning, China. *Canadian Journal of Earth Sciences* 40:731–747.
- Zhou, Z.-H., and F.-C. Zhang. 2005. Discovery of an ornithurine bird and its implication of Early Cretaceous avian radiation. *Proceedings of the National Academy of Sciences of the United States of America* 102:18998–19002.
- Zhou, Z.-H., and F.-C. Zhang. 2006. A beaked basal ornithurine bird (Aves, Ornithurae) from the Lower Cretaceous of China. *Zoologica Scripta* 35:363–373.
- Zhou, Z.-H., J. Clarke, and F.-C. Zhang. 2008. Insight into diversity, body size and morphological evolution from the largest Early Cretaceous enantiornithine bird. *Journal of Anatomy* 212:565–577.

Submitted July 3, 2009; accepted December 21, 2009.